The role of LBD proteins in floral organ abscission

Ingerid Ørjansen Kirkeleite

Thesis for the Degree Master of Science
60 study points

UNIVERSITY OF OSLO
Faculty of Mathematics and Natural Science
Department of Biosciences

Acknowledgements

The work presented in this thesis was carried out at the Department of Biosciences, Faculty of Mathematics and Natural Sciences University of Oslo, in the period between January 2013 and August 2014, Supervision has been provided by Professor Reidunn B. Aalen (formal supervisor), Research fellow Melinka A. Butenko and Post doc. Chun-Lin Shi.

First I would like to thank Professor Reidunn B. Aalen for the opportunity to do my master thesis in her research group and Research fellow Melinka A. Butenko for including me in her research project. I am grateful for all the skilled guidance and supervision in the process of working out my master thesis.

Many thanks to Post doc. Chun-Lin Shi for all the help in the lab and during the writing of my thesis.

Thanks to Ph.D. student Mari Wildhagen for reading my master thesis and for always being so cheerful. Thanks also to Post doc. Ullrich Herrmann for gladly lending a hand and for all the nice conversations.

I wish to thank Solveig Hauge Engebretsen and Roy Fallet for always lending a smile and a helping hand in the lab and in the phytotron.

A special thanks to Line and the other master students with whom I have had the pleasure of sharing an “office”. They have made this journey so much easier.

Finally, I want to thank all my friends and family for all their love and support, and last, but not least, special thanks to Lars-Inge, my boyfriend, for all the smiles, jokes and encouraging words I so desperately needed the last couple of weeks.

Oslo, August 2014
Ingerid Kirkeleite

Abstract

Abscission is a developmental process where plant organs are actively shed from the plant body either due to infection or simply because the organ no longer serves a purpose for the plant. In *Arabidopsis thaliana* (Arabidopsis) floral organs are shed after pollination in a cell separation event that has been shown to be controlled by the INFLORECENCE DEFICIENT IN ARABIDOPSIS (IDA) peptide through the two receptor-like kinases, HAESA and HAESA-LIKE2. IDA activates a MITOGEN-ACTIVATED PROTEIN KINASE (MAPK) cascade inducing cell separation in the abscission zone (AZ). The MAPK cascade, again, is believed to regulate three *Arabidopsis* KNOX homeodomain transcription factors (TF), *KNAT1* which inhibits cell wall loosening and controls *KNAT2* and *KNAT6* which induce cell separation. During leaf development *KNOX* genes have been implicated to be directly repressed by a complex consisting of ASYMMETRIC LEAVES 1 a member of the HLH family and ASYMMETRIC LEAVES2, a member of the LATERAL ORGAN BOUNDARIES DOMAIN (LBD) family. Another LBD protein, JAGGED LATERAL ORGAN (JLO), is also involved in *KNOX* regulation when coordinating organ development in shoot and floral meristems. JLO and AS2 can together with AS1 form trimeric complexes to suppress *KNAT1* expression during lateral organ development. We recently showed that two other members of the LBD family, *LBD37* and *LBD39*, are up-regulated in *ida* and *hae hsl2* mutants, indicating that members of the LBDs are being down-regulated in the IDA signalling pathway. We propose that IDA signalling negatively regulates the LBDs in abscission zone cells, preventing the LBDs from down-regulating *KNAT2* and *KNAT6*, this in turn allowing these TFs to induce floral organ abscission. Here, we will explore the possibility of this proposed model by investigating single and higher order mutants of four closely related *LBD* genes, including *LBD37* and *LBD39*, their expression pattern during floral organ abscission, and by determining their genetic interactions with *KNAT2*, *KNAT6*, *IDA* and *HAE HSL2*.

Table of Contents

Table of Contents

1 Introduction

1.1 Arabidopsis as a model organism

Arabidopsis is a small robust flowering plant from the mustard family (Meinke et al., 1998). Due to its physical traits, short generation time (about six weeks), self-pollination and its ability to produce a large number of seeds Arabidopsis has been a first choice of study of many plant biologists. In addition, Arabidopsis is easily transformed by the *Agrobacterium tumefaciens*, which can transfer its T-DNA into the plant cell where the T-DNA integrates into the plant genome (Clough et al., 1998).

In 2000 Arabidopsis was the first plant ever to get its genome fully sequenced.
The genome consists of 125Mega bases constituting one of the smallest genomes in the plant kingdom (Arabidopsis Genome Initiative, 2000).
The genome is organized into five chromosomes containing around 25,500 genes (Arabidopsis Genome Initiative, 2000).

Arabidopsis has been shown to be a suitable model organism for investigating an extensive number of essential developmental processes in plants. Abscission, the programmed loss of plant organs, is important during plant development and Arabidopsis has proven to be a suitable system for studying this process as the characteristics for floral organ abscission are similar to that of other abscission processes found in other plant species like beans and tomatoes (Bleecker and Patterson, 1997; Patterson, 2001). In addition, the presence of progressive older flowers and siliques from unfertilized buds to mature siliques along the length of a single inflorescence makes Arabidopsis useful for following the different stages of floral abscission and the changes that the cells undergoing separation go through.

1.2 Cell separation in plants

A number of cell separation events take place at different developmental stages during the life cycle of a plant and are caused by the breakdown of the pectin rich matrix that connects adjacent cells preceded or followed by cell wall remodeling (Roberts et al., 2002; Jarvis et al., 2003). Cell separation is a process important for the plants reproductive success, shattering of infected organs or organs that have served their purpose for the plant as well as for architectural alterations of the plant body. The different sites at which cell separation can occur are displayed in figure 1.1 and include shattering of pods and shedding of germinated seeds as well as the seed germination itself, pollen release, shedding of organs and different tissues, and emergence of lateral roots (Roberts and Roberts, 2000; Roberts et al., 2002; Swarup et al., 2008). Cell separation has also been observed at the root tip where the peripheral cells are sloughed off as the root makes its way through the soil (del Campillo et al., 2004).

The physiological aspects taking place during the different cell separation processes share common cellular and cell wall changes and the signaling processes initiating the different separation events are believed to be conserved. Still, there are likely different environmental and biological regulatory factors that initiate the different cell separation processes so that cell separation only occurs at specific locations at suitable times. From an agricultural perspective delayed cell separation has always been an advantageous trait for avoiding preharvest shedding of fruits and seeds and to prolong the time pollination can take place to increase crop yields and quality (Pickersgill, 2007).

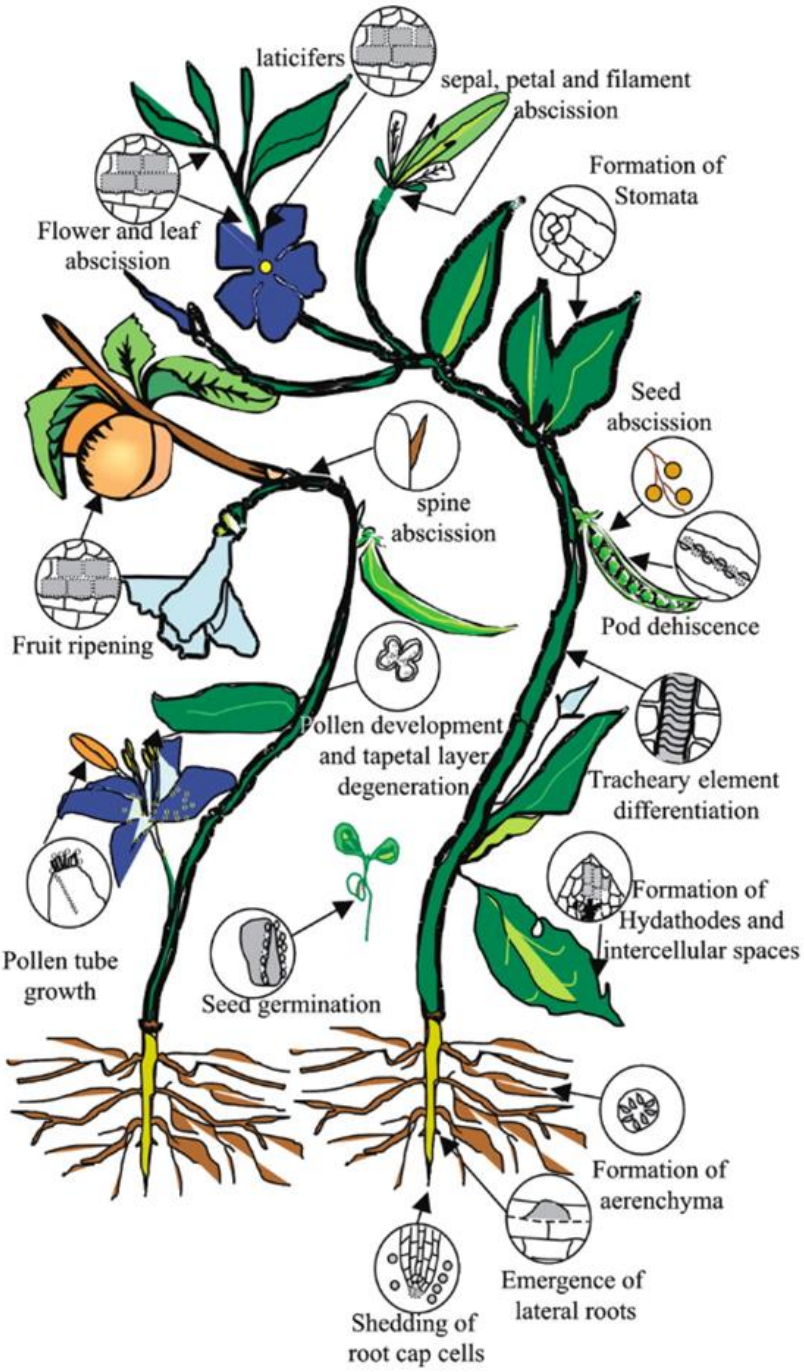

Figure 1.1: The different sites where cell separation processes may occur in plants. (Roberts et al., 2002).

1.2.1 Abscission

Abscission is the term used for processes leading to plants shedding their organs. Organ abscission is important for the plant in the removal of infected, dead or non-functional organs, but also healthy organs no longer serving a function as well as shedding of fruit and seeds (Sexton et al., 1982; Bleecker and Patterson, 1997). The position at which organ shedding takes place is called the abscission zone (AZ) (Sexton et al., 1982; González Carranza et al., 1998; Taylor et al., 2001). The AZ is located between the shedding organ and the plant body. It is characterized as several cell layers consisting of small cytoplasmically dense cells that fail to enlarge like the surrounding cells until developmental and environmental conditions trigger the initiation of abscission (Bleecker and Patterson, 1997; Roberts et al., 2002). Once triggered, there is an up-regulation of genes encoding hydrolyzing enzymes like expansins (EXP) and xyloglucan endotransglucosylase/hydrolase (XTH) which lead to a restructuring of AZ cell walls allowing for an expansion of the cells (Cosgrove, 1998; Cai and Lashbrook, 2008; Ogawa et al., 2009). Subsequently pectin-hydrolysing enzymes like polygalacturonase (PG) cause dissolution of the middle lamella as pectin gets demethylated causing a fracture plane in the separating layer (Sexton et al., 1982; González-Carranza et al., 2007; Cai and Lashbrook, 2008; Ogawa et al., 2009).To avoid pathogen invasion and loss of water and nutrients a corky layer forms across the stem as the organ detaches (Patterson, 2001).

Changes in the levels of hormones like ethylene and auxin are important in regulation of the timing of abscission as ethylene activates abscission while auxin delays abscission by making the AZ cells less responsive to ethylene (Osborne et al., 1989; Taylor et al., 2001). However, indoleacetic acid (IAA), a member of the auxin class of plant hormones, is not only important for timing but also for the rate at which the cell wall is degraded and the need for a functional IAA signaling pathway for organ abscission to take place have recently been demonstrated (Basu et al., 2013). In lateral root emergence (LRE) auxin influx has been shown to be the starting point of the process of separating cell layers overlaying the incipient lateral root further expanding the role of auxin in cell separation processes (Kumpf et al., 2013).

1.2.2 Floral organ abscission

Floral organ abscission is the process where floral organs like petals, stamen and sepals are abscised from the floral AZ, which is believed to derive from the floral meristem (Gawadi, 1950; Patterson, 2001; van Nocker and van, 2009). In Arabidopsis the floral organs are shed after pollination at a time where the floral organs have served their purpose for the plant (Patterson, 2001). The knowledge of the different genes regulating the process of floral abscission is steadily increasing, and has challenged the role of classical plant hormones, like ethylene and auxin, as the most important regulators of plant development (Butenko et al., 2009; Stahl et al., 2010).

In Arabidopsis BLADE-ON-PETIOLE1 (BOP1) and BOP2, two NPR1-like signaling proteins with conserved BTB/POZ domain and ankyrin repeats (Hepworth et al., 2005; McKim et al., 2008) have been found to play a role in promoting differentiation of floral organ AZ cells (figure 1.2) as loss of BOP1 and BOP2 function prevents proper structural formation of AZ cells and *bop1 bop2* show no sign of weakening of the petals (McKim et al., 2008).

The INFLORESCENCE DEFICIENT IN ABSCISSION (IDA) peptide has been found to be involved in the final step of abscission (Figure 1.2) where the actual cell separation by dissociation of cell walls occurs as the *ida* mutant show maturation of the AZ, but organ shedding does not take place (Butenko et al., 2003). *IDA* is expressed shortly after sensitization of the AZ and seems to be involved in cell wall loosening prior to organ detachment, and display precocious floral organ abscission and an enlargement of AZ cells at the point of organ detachment when overexpressed (Butenko et al., 2003; Butenko et al., 2006; Stenvik et al., 2006). Earlier and epistatic expression of *IDA* could not promote abscission in *bop1 bop2* (McKim et al., 2008). Thus, the presence of atomically differentiated AZ cells most likely provided by BOP1 and BOP2 are essential for the IDA peptide to promote floral organ abscission (McKim et al., 2008; Shi et al., 2011).

Another gene called *NEVERSHED (NEV)*, a ADP-ribosylation factor GTPase-activating protein located in the trans-Golgi network, is thought to act at the same stages as IDA regulating abscission (Figure 1.2) (Liljegren et al., 2009). Loss of *NEV* displays deficient abscission of floral organs and causes like overexpression of *IDA* ectopic expansion of the AZ cells (Liljegren et al., 2009; Liu et al., 2013). Transmission electron micrographs revealed

altered Golgi structure and location of the Golgi network in the sepal AZs of *nev* mutants and genes suggested to be involved in cell separation were found to be downregulated in *nev* mutants (Liu et al., 2013). Thus NEV likely regulates membrane trafficking sustaining a proper organization of the Golgi apparatus and correct localization of the Golgi network important for the progression of abscission and cell separation (Liljegren et al., 2009; Stefano et al., 2010). Taken together NEV seems to act as an inhibitor of cell expansion while IDA promotes it, whereas both NEV and IDA are needed for the promotion and proper execution of cell separation(Butenko et al., 2003; Butenko et al., 2006; Stenvik et al., 2006; Liljegren et al., 2009; Liu et al., 2013).

HAESA (HAE) and HAESA-LIKE 2 (HSL2), two leucine-rich repeat-receptor-like kinase (LRR-LRK), are involved in the promotion of abscission as receptors for the IDA peptide transducing its signal to cytoplasmic effectors (Cho et al., 2008; McKim et al., 2008; Stenvik et al., 2008; Butenko et al., 2009; Butenko et al., 2014). EVRSHED (EVR), CAST AWAY (CST) and SOMATIC EMBRYOGENESIS RECEPTOR-LIKE KINASE1 (SERK1) on the other hand are the three receptor-like kinases implied to work as spatial inhibitors of abscission by preventing abscission activation (Leslie et al., 2010; Lewis et al., 2010; Burr et al., 2011). Mutations in *EVR, CST* and *SERK1* have the ability to restore the trans-Golgi network and organ abscission in *nev* (Leslie et al., 2010; Lewis et al., 2010; Burr et al., 2011). In fact mutations of *CST, EVR* and *SERK1* in *nev* lead to precocious abscission and enlargement of AZ layer supporting their role as negative regulators of abscission (Leslie et al., 2010; Lewis et al., 2010; Burr et al., 2011). However, *evr, serk1* and *cst* alone does not display any visible abscission defects and were unable to rescue *ida* and *haehsl2* abscission defects suggesting they act in a different pathway than IDA (Leslie et al., 2010; Lewis et al., 2010; Burr et al., 2011). Even so, it has been suggested that EVR, CST and SERK1 are able to block the IDA signal by forming a complex with HAE HSL2 prior to ligand binding triggering internalization and recycling of the receptors via endocytosis regulated by the NEV molecule (Liljegren et al., 2009; Burr et al., 2011; Liu et al., 2013).

BREVIPEDICELLUS (BP)/ KNOTTED-LIKE FROM ARABIDOPSIS THALIANA1 (KNAT1) a member of the *KNOTTED-LIKE HOMEODOMAIN (KNOX)* gene family, are proposed to play an important role in proper timing and regulation of the enlargement of morphologically distinct AZ cells in floral organ abscission (Figure 1.2) (Wang et al., 2006; Shi et al., 2011). Loss of *KNAT1* activity, as with gain of IDA function leads to enlargement of AZ cells and

early cell wall loosening at the positions where shedding of the floral organs take place (Shi et al., 2011). Two other *KNAT* genes (*KNAT2* and *KNAT6*) are believed to be promoters of abscission by direct activation of *Cell Wall Remodeling (CWR)* genes and are in turn suggested to be regulated by BP/KNAT1 (Ragni et al., 2008; Shi et al., 2011). KNAT1 may also restrict cell expansion and proliferation through activation of *EVR*, as *EVR* is downregulated in *knat1* mutants (Shi et al., 2011), though, likely in an IDA independent manner suggesting the involvement of other genes in the interconnected pathways (Leslie et al., 2010).

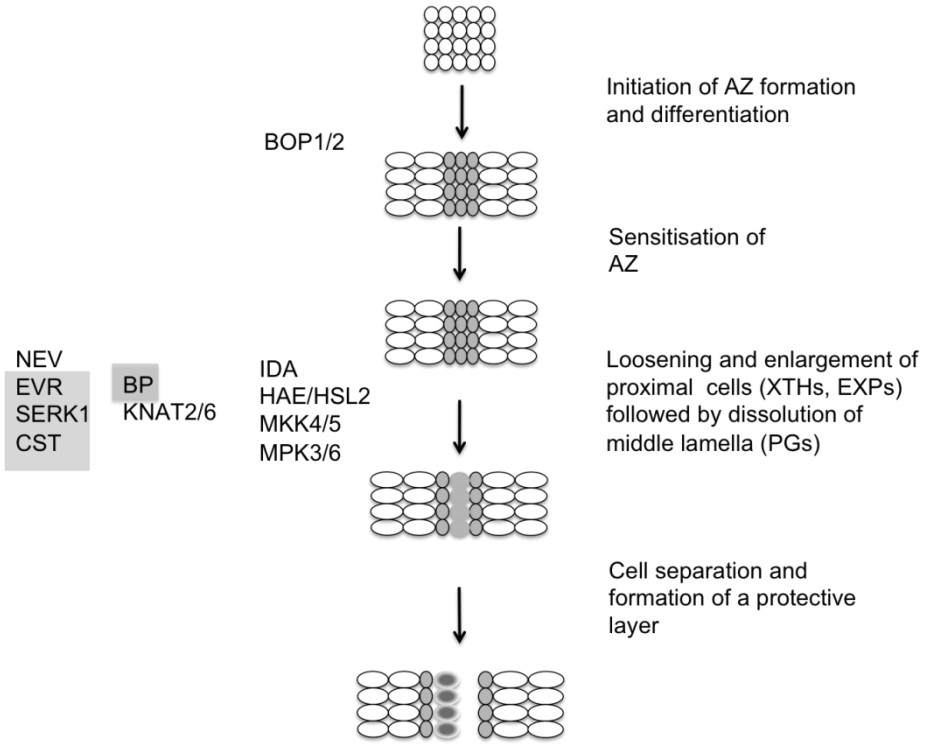

Figure 1.2 Model of floral organ abscission in Arabidopsis. The events and the genes acting in floral organ abscission from AZ formation to cell separation are demonstrated here. On the left the genes involved in initiation of AZ formation and differentiation, activation of cell wall loosening, dissolution of middle lamella are listed. Genes involved in the latter remain active or actively repressed throughout the cell separating process. (Gray boxes mark inhibitors of abscission.) On the right the physiological aspects is briefly described also including some of the central enzymes enacting in cell wall loosening and dissolution of the middle lamella. Modified from Patterson (2001), Liljegren et al., (2012) and Aalen et al., (2013).

1.3 IDA signaling pathway

Many of the different genes found to act in floral organ abscission also act in the same pathway. One of the most well studied signaling pathways leading to loss of floral organs as well as cell separation during LRE is the IDA signaling pathway where IDA and its HAE HSL2 receptors constitute the starting point (figure 1.3) (Cho et al., 2008; Stenvik et al., 2008; Butenko et al., 2009). IDA was found during a screening for delayed abscission as a recessive gene encoding a peptide regulating floral organ abscission in an ethylene-independent manner (Butenko et al., 2003). Lack of functional IDA peptide causes all the floral organs to remain attached to the abscission zones of the siliques (Butenko et al., 2003). HAE and HSL2 are expressed at the AZ of floral organs in a pattern similar to that of the IDA peptide and show the same phenotype when mutated as the *ida* mutant (Jinn et al., 2000; Butenko et al., 2003).

IDA is highly likely a small post-translationally modified peptide secreted from the AZ cells with an ability to bind HSL2 and HAE although cells of the responding tissue might need higher concentrations of HAE due to its low affinity (Butenko et al., 2003; Stenvik et al., 2006; Stenvik et al., 2008; Matsubayashi, 2011; Butenko et al., 2014). Proper downsizing and modifications of the 77 aas long polypeptide encoded by the *IDA* gene is required for gaining a fully active peptide (Matsubayashi, 2011). PIP, a 12 aas long part of the 20 aas long conserved proline-rich C-terminal domain of IDA termed the Extended PIP (EPIP) motif and even more so hydroxylated PIP on at least the 7^{th} pro have been shown to have high affinity for the HSL2 receptor in a bioassay using oxidative burst (Butenko et al., 2014). PIP and PIPPo could not as efficiently activate HAE and further modifications of IDA or even the presence of a coreceptor may be necessary for binding to the HAE receptor (Butenko et al., 2014).

Genes encoding INFLORESCENCE DEFICIENT IN ABSCISSION-LIKE (IDL) 1-5 peptides have been found during bioinformatic screenings all sharing a conserved EPIP motif and are therefore also likely to act as signaling peptides binding RLKs (Stenvik et al., 2008). *IDL* genes are like *IDA* expressed in AZ, however, *IDL* expression peaks after organ shedding in contrast to *IDA* suggesting separate functions from IDA (Stenvik et al., 2008).

HAE HSL2 are thought to initiate transduction of the IDA signal via a Mitogen-Activated Protein Kinase (MAPK) cascade in the cytoplasm (figure 1.3) that includes Mitogen-Activated Protein Kinase4 (MKK4) and MKK5 and their two known targets Mitogen-

Activated Protein Kinase 3(MPK3) and MPK6 (Tena et al., 2001; Cho et al., 2008; Kim et al., 2011). MKK4 and MKK5 when constitutively expressed could rescue the phenotype of *ida* and *hae hsl2* and *MPK6* transgene together with *mpk3* mutant showed deficiency in abscission giving them a role as positive regulators of abscission in the IDA-HAE HSL2 pathway (Cho et al., 2008). The activation of MAPK cascade is believed to directly or indirectly down regulate KNAT1 found to function downstream of IDA and HAE HSL2 (Shi et al., 2011). Genetic interaction studies suggest a role of KNAT1 as a negative regulator of abscission acting downstream of IDA peptide and HAE HSL2 receptors negatively regulating *KNAT2* and *KNAT6* (figure 1.3) (Shi et al., 2011). Both *knat2knat6* and *bp-3ida-2knat2knat6* mutants show delayed abscission and the absence of *KNAT6* and *KNAT2* can rescue the *knat1* phenotype of downward-pointing siliques supporting a role for KNAT2 and KNAT6 downstream of KNAT1 (Ragni et al., 2008; Shi et al., 2011). Furthermore, the expression level of *KNAT2* and *KNAT6* are elevated in *knat1* mutants, while in *ida* and *haehsl2* mutants the expression levels are almost abundant compared to wild type (Shi et al., 2011). This further supports the hypothesis of KNAT2 and KNAT6 acting as positive regulators of abscission by induction of *Cell Wall Remodeling (CWR)* genes as a downstream effect of the action of IDA and HAE HSL2 (Shi et al., 2011).

More recent studies have shown that IDA-HAEHSL2 signaling also is important in the cell separating processes of LRE (Kumpf et al., 2013). Kumpf et. al. (2013) demonstrated that auxin influx could induce *IDA* in overlaying endodermal (EN), cortical (CO) and epidermal (EP) layers which then by signaling through HAE HSL2 caused activation of *CWR* genes encoding cell wall remodeling enzymes causing dissolution of that middle lamella between cells of the EN, CO and EP layers enabling the emergence of the LR (Kumpf et al., 2013).

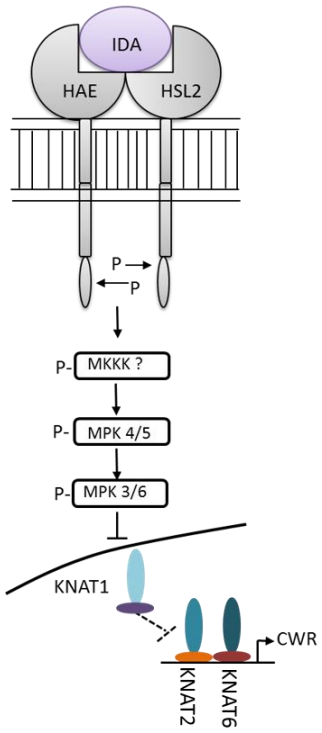

Figure 1.3: The IDA signaling pathway. The IDA signaling pathway so far involves signaling by IDA through HAE HSL2 causing activation of a MAP cascade that leads to the repression of KNAT1 leaving KNAT2 and KNAT6 active and able to activate transcription of *CWR* genes. The stippled line represents the uncertainties involving the regulation of *KNAT2* and *KNAT6* by KNAT1. The figure is modified from Shi et al., (2011).

1.4 The LBD family of transcription factors

In addition to their involvement in floral organ abscission, BP/KNAT1, KNAT2 and KNAT6 have previously been demonstrated to be required for meristem maintenance and organ patterning (Bürglin, 1997; Müller et al., 2001). Recent studies have found several members of the *LATERAL ORGAN BOUNDARIES Domain* (*LBD*) Gene Family to be involved in the regulation of the same *KNOX* genes during plant development (Semiarti et al., 2001; Borghi et al., 2007; Guo et al., 2008; Rast and Simon, 2012). LBDs, which often work as heterodimers, have been shown to act as transcription factors in various developmental processes controlling plant architecture and growth working with other LBDs when regulating their targets (Semiarti et al., 2001; Shuai et al., 2002; Xu et al., 2003; Borghi et al., 2007; Rast and Simon, 2012). In the last decade several LBDs have been characterized further increasing the knowledge about the LBD family.

The LBD family of Arabidopsis consists of 43 members, all of which contain a 100 amino acid long Zinc finger-like domain with a conserved 4 Cys motif ($CX_2CX_6CX_3C$) and a conserved Pro residue constituting the LATERAL ORGAN BOUNDARIES domain (LOB-domain) (figure 1.4) (Iwakawa et al., 2002; Shuai et al., 2002). The LBD family is a plant specific family of transcription factors divided into Class I and Class II where 37 of the total 43 members constitute Class I where the similarities between the members are generally higher that between the six members of Class II (Shuai et al., 2002).

33 of the 37 members in the Class I of LBD genes are predicted to form a coiled-coil structure at the end of the LOB domain where four Leucines with the spacing $LX_6LX_3LX_6L$ resembling a Leucine Zipper are found (Iwakawa et al., 2002; Shuai et al., 2002). Leucine Zippers in general are involved in protein-protein interactions suggesting that the coiled coil of the LBDs also mediate association with other proteins (Ellenberger et al., 1992). None of the Class II members, however, are predicted to have this coiled-coil suggesting a different function. An expression study of all the predicted *LBD* gene family members (Shuai et al., 2002), shows expression of *LBD* genes in a variety of tissues suggesting the involvement of LBDs in many different plant specific processes as LBDs are only found in plants (Shuai et al., 2002; Kawade et al., 2013). Further supporting the diverse roles of LBDs in plant specific development are their involvement in embryogenesis, organ formation and organ boundary definition (Shuai et al., 2002; Xu et al., 2003; Borghi et al., 2007; Okushima et al., 2007; Rast and Simon, 2012).

The LOB domain has a DNA binding activity that binds cis-element 5'-GCGGCG-3' giving LBD proteins the ability to form dimers with other LBDs as well as basic Helix-Loop-Helix (bHLH) family members, supporting the involvement of LBDs in protein-protein interactions (Husbands et al., 2007; Guo et al., 2008; Rast and Simon, 2012). This activity seems conserved through the entire LBD family of Arabidopsis as even LBD41 from Class II has this activity (Husbands et al., 2007).

Phylogenetic analysis showed high similarity in the LOB domain of various LBDs and RT-PCR revealed overlapping expression indicating redundancy amongst the LBDs (Shuai et al., 2002). However, one LOB domain cannot substitute a LOB domain of another closely related LBD as a LOB domain swap revealed that varying amino acid within the domain are responsible for the function of the different LBDs (Mangeon et al., 2012).

Figure 1.4: LOB domain of class II LBDs in comparison to the LOB domain of LOB from Class I. The gray area marks the LOB domain of the class II LBD members (LBD37 - LBD42) and the LOB of class I, the C block with the $CX_2CX_6CX_3C$ domain is marked by a black underscore, the Cys residues and the conserved Prolin are marked by a black spot. Finally, each of the four leucines present in the LOB domain of *LOB* is marked with a underscore.

1.4.1 LBDs negatively regulate Class I KNOTTED-Like Homeobox Proteins

Plant meristems are crucial for plant growth and organ development at early and later developmental stages. KNOX proteins are found to be involved in meristem maintenance actively preserving a pool of undifferentiated cells residing within the meristems from which organ primordia derive (Barton and Poethig, 1993; Long et al., 1996; Byrne et al., 2002). Upon organ formation and differentiation, repression of *KNOX* genes in cells determined for differentiation is important for the development of organs (Byrne et al., 2000; Ori et al., 2000; Semiarti et al., 2001; Xu et al., 2003). ASYMMETRIC LEAVES 2 (AS2) and JAGGED LATERAL ORGANS (JLO) are two LBDs found to act as negative regulators of *KNOX* genes important for the establishment of boundaries between organs (figure 1.5) (Semiarti et al., 2001; Byrne et al., 2002; Shuai et al., 2002; Xu et al., 2003; Borghi et al., 2007; Guo et al., 2008; Rast and Simon, 2012). *AS2* is expressed in leaf primordia where it repress *KNAT1* during leaf development giving developing leaves their adaxial identity (Lin et al., 2003; Mele et al., 2003), by acting in a complex with ASYMMETRIC LEAVES 1, a MYB domain containing transcription factor (and a member of the HLH family) (Barton and Poethig, 1993;

Byrne et al., 2000; Ori et al., 2000; Xu et al., 2003; Guo et al., 2008). Binding of AS2 to AS1 enables the binding of AS1 to the *KNOX* promoter region likely causing the formation of a repressive loop and chromatin remodeling complexes such as HIRA and Polycomb-repressive complex 2 (PRC2) are recruited (Phelps Durr et al., 2005; Guo et al., 2008; Lodha et al., 2013). PRC2 then induce a repressive chromatin state which is likely inherited through several cell divisions during leaf development as expression of AS1 and AS2 only overlap in young leaf primordia (Byrne et al., 2000; Xu et al., 2003; Phelps Durr et al., 2005; Guo et al., 2008; Lodha et al., 2013).

JLO are expressed in organ initiation sites and later in the boundaries between the Shoot Apical Meristem (SAM) and lateral organ primordia regulating the KNOX members *SHOOT MERISTEMLESS (STM)* important for SAM formation and maintenance and *KNAT1* during lateral organ development (figure 1.5) (Borghi et al., 2007; Rast and Simon, 2012). Loss-of-function studies of JLO showed expanded expression of *STM* and *KNAT1* across the base of lateral organ primordia in *jlo* indicating JLO as a negative regulator restricting *KNAT1* and *STM* expression beyond SAM (Rast and Simon, 2012). In vivo analysis showed the ability of AS2 to bind to JLO, which could mediate the binding of JLO to AS1 as well (Rast and Simon, 2012). However, AS2 and JLO are also believed to act independently of AS1 as *AS1* and *AS2* show different phenotypical abnormalities when overexpressed and have overlapping but not identical expression pattern (Byrne et al., 2002; Iwakawa et al., 2002; Iwakawa et al., 2007; Rast and Simon, 2012). Thus, JLO can relay its restrictive constrains on *KNOX* during plant development as part of a tetrameric complexes with AS2 and AS1 or a heteromeric complexes with AS2 or by forming a homomer (Rast and Simon, 2012).

Another in vivo study revealed that another LBD family member, LBD31, could interact with both AS2 and JLO (Rast and Simon, 2012). LBDs are obviously capable of forming complexes with each other as well as other transcription factors resulting in different binding abilities to different targets.

1.4.2 LBDs are in turn regulated by BOPs

In addition to regulate AZ formation BOP1 and BOP2 are important for leaf morphogenesis and patterning (Ha et al., 2003; Ha et al., 2007). BOP1 and BOP2 share distinct and overlapping expression and in vivo studies demonstrated their ability to dimerize (Norberg et al., 2005; Jun et al., 2010). BOP1 and BOP2 have been shown to be important for *KNOX* repression during leaf development as phenotypical defects of *bop1 bop2* mutants are likely to be a result of ectopic *KNOX1* expression (*KNAT1*, *KNAT2* and *KNAT6*) as well as *YABBY* (*YAB*) expression, which is most likely important for maintaining the adaxial-abaxial polarity (Siegfried et al., 1999; Ha et al., 2003; Ha et al., 2007; Sarojam et al., 2010).

In vitro and in vivo studies show that BOP1 and BOP2 act as transcriptional activators of *AS2* as demonstrated in figure 1.5 by direct binding of BOP1 to *AS2* promoter region thus indirectly suppressing *KNOX1* genes (Ha et al., 2010; Jun et al., 2010). Furthermore, genetic studies of *stm* embryos showed that ectopic expression of *AS2* was dependant on active BOP (Jun et al., 2010). Other *LBDs* induced by BOP1 and BOP2 are *LOB* (figure 1.5), which can be directly activated by AS2-AS1 complex, and LBD36 both responding positive to increasing expression levels of *BOP1* and *BOP2* (Ha et al., 2007). However, BOP1 and BOP2 can also cause repression of *KNOX* genes in an AS2 independent manner as *knox1* to some extent can rescue *bop* but not *as2* phenotype (Ikezaki et al., 2010; Jun et al., 2010).

In inflorescence KNAT1 and PENNYWISE (PNY) are in turn believed to act as repressors of *BOP1* and *BOP2* as well as *KNAT6* thus preventing premature cell differentiation and shortened internodes indicating that the timing of repression of *KNOX* is important for proper development (Ragni et al., 2008; Khan et al., 2012). Both inactivation of *KNAT6* and *BOP1/2* are able to partially rescue the defects of *knat1* and *pny* placing KNAT6 and BOP1/2 in the same signaling pathway regulating inflorescence architecture and perhaps other pathways such as the IDA signaling pathway where KNAT1 also act as a repressor of *KNAT6* inhibiting floral organ abscission (Ragni et al., 2008; Shi et al., 2011; Khan et al., 2012).

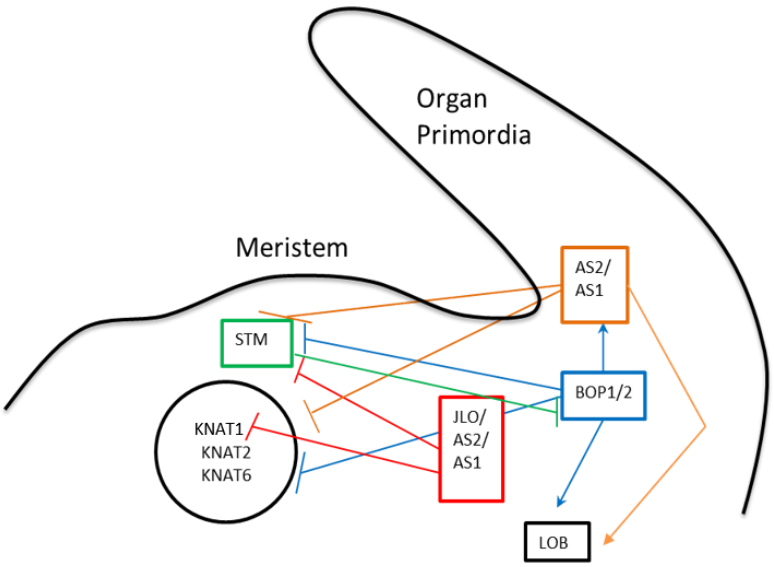

Figure 1.5: Simplified model of the genetic network underlying meristem patterning, organ-to-meristem boundary domain formation and organ initiation. Arrows and inhibition lines represent positive and negative regulations, respectively. LOB and the tetrameric complex JLO/AS2/AS1 are active in the meristem-to-organ boundaries. Expression of LOB is regulated by BOP1/2 which also positively regulates AS2/AS1. JLO/AS2/AS1 acts as a suppressor of *KNOX* genes in the boundaries between meristem and organ primordia. AS2/AS1 is active in the organ primordia where it interacts with chromatin remodeling complexes to ensure repression of *KNOX* gene expression. Ha et al., (2010), Jun et al., (2010) and Žádníková (2014).

1.4.3 LBD37, LBD38, LBD39 and LBD41

LBD37, *LBD38* and *LBD39* arose most likely from two segmental duplications of the Arabidopsis genome (http://www.tigr.org/). LBD37, LBD38, LBD39 and LBD41, members of the Class II of the LBD family, are closely related LBDs belonging to the same cluster (Shuai et al., 2002). *LBD38* and *LBD39* are predicted to co-express in Arabidopsis thaliana and the LBD37 protein are found to be localized in the nucleus further supporting the role of LBDs as transcription factors (Rubin et al., 2009). *LBD37*, *LBD38* and *LBD39* have shown to be inducible by Nitrogen and thereby acting together as repressors of nitrogen responsive genes like *PAP1/PAP2* causing a decrease in Anthocyanin synthesis (Rubin et al., 2009).

Interestingly, data provided by Meng et. al. (2010) show that LBD41 also localizes to the nucleus functioning as a transcription factor involved in determination on adaxial-abaxial identity in lateral organ development in the plant cockscomb (Celosia cristata) possibly

through regulations of KNOX members as malformed leaves and flowers seen in *35S:LBD41* probably were caused by misexpression of cockscomb *KNOX* genes (Meng et al., 2010).

In a yeast two-hybrid experiment LBD37 and LBD41 were found to interact with TOPLESS (TPL) and TOPPLESS-related (TPR) corepressors from the TPL/TPR family of Groucho/ Tup1-like corepressors (Causier et al., 2012). This opens a possibility of LBDs interacting with different cofactors as well as other TFs when relaying their regulatory constraints (Husbands et al., 2007; Causier et al., 2012).

As LBDs have been shown to be able to regulate *KNOX* genes in different plant developing processes and as LBD41 has been indicated a role as *KNOX* repressor in cocscomb it would be interesting to investigate the possibility of these four closely related LBDs acting as regulators of *KNOX* genes in floral organ abscission in Arabidopsis.

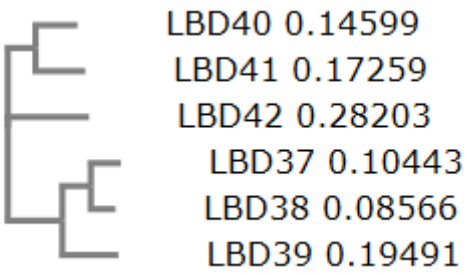

Figure 1.6: Phylogenetic tree over members of the LBD family class II. Genetic distance is included indicating the high degree of similarity between the class II LBD members.

1.5 Aim of study

In this study, we wanted to investigate the possibility of LBD37, LBD38, LBD39 and LBD41 acting in floral organ abscission. We propose here that the *LBDs* are negatively regulated upon the transduction of the IDA signal. This would inhibit them from suppressing class 1 *KNOX Homeobox* genes facilitating induction of floral organ abscission through activation of *Cell Wall Remodeling (CWR)* genes (figure 1.7). To test this proposed model and potential floral organ abscission related phenotypes single and double *lbd* mutant lines were made. Different expression constructs were made in order to investigate the temporal and spatial

expression pattern of the LBDs. In addition, we wanted to examine the potential link between LBDs and factors of the IDA signaling pathway through genetic interaction studies by looking at the expression pattern of *LBDs* in *ida* and *haehsl2*. Furthermore, the potential rescue of the *hae hsl2* phenotype by loss-of-*LBDs* was investigated. Finally, since negative regulation of *KNOX* genes by LBDs promotes differentiation of meristematic cells, the expression pattern and expression level of *KNOX* genes in *lbd* single mutant lines were analyzed.

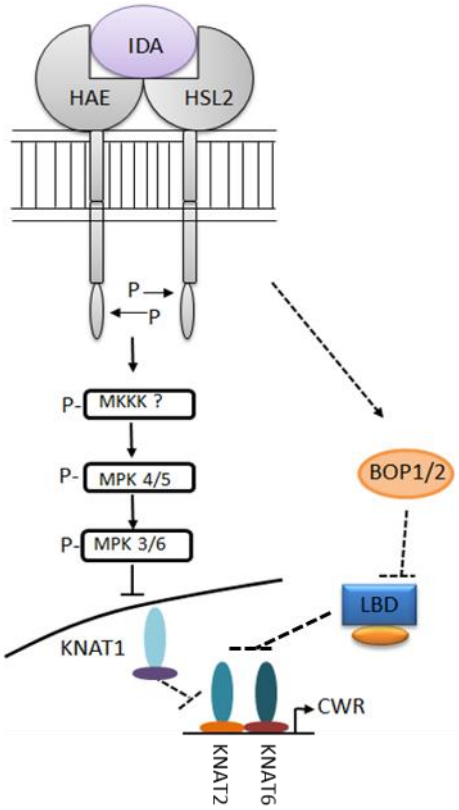

Figure 1.7: Proposed model of IDA signaling pathway including LBD as inhibitor of abscission by repressing KNOX activity. The stippled lines symbolize regulatory interactions that not yet have been confirmed. In this model IDA repress *KNAT2* and *KNAT6* through a proposed additional pathway where IDA positively regulates *BOP1/2* which cause repression of *LBDs*, thus disabling repression of *KNAT2* and *KNAT6* leading to *CWR* gene expression. Modified from Shi et al., (2011).

2 Materials and Methods

2.1 RNA and DNA techniques

2.1.1 Isolation of genomic DNA

Genomic DNA, used to quantify promoter regions of *LBD37*, *LBD38*, *LBD39* and *LBD41* and as genomic control, was isolated following a protocol modified after Dellaporta et. al (1983). 20 milligrams (mg) of tissue from rosette leaves and sprouts were harvested from Colombia (Col) wild type (wt) and immediately frozen in liquid nitrogen ((l)N_2). The frozen tissues were crushed using a mortar. Preheated (65 °C) Elution buffer (EB) (100 mM Tris-HCl pH 8.0, 50 mM Ethylenediaminetetraacetic acid (EDTA) pH 8.0, 0.5 M NaCl, 1.25 % SDS, 8.3 mM NaOH, and 0.38 % Na bisulfate) containing mercaptoethanol (2-ME) (66 µl per 100 ml EB) was added. The solutions were transferred to corex tubes and incubated at 65 °C with occasional stirring. After 10 minutes (min) 5 ml 3 Molar (M) Potassium acetate (KAc) was firmly added and the solutions were left on ice for 20 min followed by a 10 min centrifugation at 4 °C, 10 000 revolutions per min (rpm), using a TJ-25 centrifuge (Beckman Coulter, Inc.) with a TS-5.1-500 rotor. Supernatants were filtered through mira cloth into a new corex tube with isopropanol and left to precipitate for 1 hour (h) at room temperature (RT) followed by a 20 min centrifugation at 4 °C, 10 000 rpm. The pellets were cleansed in 70 % Ethanol (EtOH) twice before resolving it in T5E (50 mM Tris-HCl pH 8.0, 10 mM EDTA) over night (O.N) at 4 °C. The day after 14 µl RNase were added to the resolved pellets and incubated at 37 °C for 1 h. 50 µl 3 M Natrium acetate (NaAc) per 500 µl of resolved pellets together with pre cooled (-20 °C) absolute alcohol (1400 µl pr. 500 µl) were added. After centrifugation supernatants were removed and pellets were cleansed twice with 70 % EtOH. When dry, the pellets were resolved in 250 µl distilled water (dH_2O) O.N at 4 °C.

2.1.2 DNA isolation with Ultraprep Genomic DNA plant Kit

For isolation of genomic DNA for genotyping Ultraprep Genomic DNA Plant Kit from AHN Biotechnologie GmbH was used and the protocol from the manufacturer was followed. 150 mg of Arabidopsis leaves were frozen in (l) N_2 before homogenization using Retch MM301(Retch GmbH). PB buffer with Proteinase K were added to the homogenized tissue and the mixture was vortexed before incubation at 52 °C for 30 min followed by a 5 min centrifugation at RT, 13 000 rpm. Clarified supernatant was transferred to a new Eppendorf tube and AB was added. The solutions were transferred to a spin column and the samples were washed with Wash Buffer (WB) and 70 % EtOH before the DNA was eluted with Elution buffer (EB) buffer.

2.1.3 RNA isolation

Isolation of RNA was done using Spectrum™ Plant Total RNA Kit (Sigma-Aldrich). As the mRNAs are quickly degraded the tissue was stored at -80 °C. Siliques at position 4, 6 and 8 along the inflorescence (position 1 representing the youngest flower with visible white petals (Bleecker and Patterson, 1997), from 10 plants were collected in Eppendorf tubes and frozen in (l) N_2. The frozen tissue was transferred to an Eppendorf tube containing small ceramic beads and 500 µl lysis solution (10 µl 2-mercaptoethanol (2-ME) for every 1mL lysis buffer) was added on ice. The tissue was crushed using a MagNAlyser (Roche) at 7000 rpm for 15 seconds (sec), followed by a cool-down at -20 °C for 2 min and finally the samples were centrifuged for 1 min at 4 °C, 13 000 rpm using a Eppendorf 5415R Refrigerated Micro Centrifuge. These steps were repeated until the tissue was completely homogenized. The sample was transferred to a sterile Eppendorf tube and centrifuged for 3 min at 4 °C, 13 000 rpm before supernatant was transferred to a Filtration column and centrifuged for 1 min at 4 °C, 13 000 rpm. Binding solution was added to the clarified flow- through and mixed by pipetting carefully before transferring the flow-through onto a Binding column. To remove any DNA On-Column DNase digestion was performed using On-Column DNase Kit (Sigma-Aldrich). 80µl of digestion solution (10 µl DNase in 70 µl DNase buffer) was added to the center of the Binding column. To remove the digested DNA the Binding column was washed with Wash solution 1 and for a final wash Wash Solution 2 diluted with EtOH was added.

When all liquid was removed, the column was transferred to a sterile 2 ml collection tube. Purified RNA was eluted with 50 µl nuclease-free water and stored at – 20 °C.

2.1.4 cDNA synthesis

After isolating the RNA it was transcribed into complementary DNA (cDNA) using SuperScript® III Reverse Transcriptase (Invitrogen). Oligo dT primers contain a poly T-tail which bind to the poly A tail in the 3'end of the mRNA. By addition of dNTP, reverse transcriptase (RT) buffer and RNase inhibitor together with RT the enzyme will reversely transcribe the mRNA into double stranded cDNA. To remove template RNA RNase H was added at the end of the inactivation of the RT enzyme.

2.1.5 Polymerase chain reaction

Polymerase chain reaction (PCR) is a fast and easy method for detecting and amplifying DNA or RNA fragments in vitro. Key components in a PCR reaction are a thermostable DNA polymerase for synthesizing the new DNA from the template, dNTPs (deoxynucleotide triphosphate), primers which provides a free 3' hydroxyl group onto which the DNA polymerase can attach new dNTP. The PCR program has several steps: denaturation of the template into single stranded DNA (ssDNA), primers annealing to the ssDNA and elongation leading to synthesis of complementary strands. Variations of a general PCR program (table 2.1) were used, varying annealing temperature depending on the primers and the annealing time, amplification temperature and amplification time depending on the polymerase used. When working with primer sets with different annealing temperature touchdown programs were used, lowering the temperature 0.2 – 0.3 °C every cycle.

The promoter region of LBD37, LBD38, LBD39 and LBD41for cloning (section 2.1.13) were amplified using proofreading polymerases, Advantage 2 polymerase (Clontech) and KOD Hot Start DNA polymerase (TOYOBO). Screening for correct insert of purified plasmid DNA (section 2.1.14) from transformed bacteria (section 2.2.2 and 2.2.3) and for Real-Time PCR of the single mutant lines Taq DNA polymerase (New England BioLabs) was used, as

proofreading abilities were not required. For genotyping of plant lines (section 2.2.12 and 2.1.2) RedExtract readyMix (Sigma -Aldrich) or Taq DNA polymerase was used. The PCR setup was done according to the manufacturers recommendations. Primers used are listed in appendix 2.

Table 2.1. Standard PCR program. The period for the amplification step depends on the rate of the polymerase and the length of the wanted product. Annealing temperature depends on the optimal binding temperature for the primers used. When doing PCR on bacterial cultures the first denature step is set to last for at least 8 min to destroy the cell membrane so the DNA is released**.**

Process, temperature (°C)	Time	Cycles
Denaturation, 95 °C	8-3 min	1
Denaturation, 95 °C	~30 sec	30-40 cycles
Annealing 55-70 °C	~30 sec	
Amplification, 68-72 °C	1-3 min	
Final extension, 68-72 °C	5-10 min	1
Hold, 4-10 °C	∞	-

2.1.6 PCR clean-up system

For cleaning of PCR products and cDNA the Wizard® SV Gel and PCR Clean-Up System (Promega) was used following the protocol provided by the manufacturer. Equal amounts of Membrane binding solution as PCR amplifications were mixed and applied onto a SV Minicolumn assembly. After centrifugation for 1 min at RT, 13 000 rpm, the column with the DNA was washed using Membrane solution twice. To remove the last traces of EtOH the samles were placed at 37 °C for 10 min. PCR products and cDNA were eluted with 50 µl and 40 µl nuclease-free water, respectively.

2.1.7 Quantitative RT-PCR

Real time quantitative PCR (RT-qPCR) allows amplification and detection of the PCR product simultaneously, and is used in gene expression analysis, miRNA analysis, genetic variation analysis and protein analysis. The qPCR machine has the amplification factors of a regular PCR machine as well as the capability to detect fluorescence light.

Expression of *KNAT1*, *KNAT2* and *KNAT6* in *lbd* single mutants and *LBD37* and *LBD39* in *ida* and *hae hsl2* mutants were measured using the LightCycler® 480 (Roche) and LightCycler®96 (Roche) following the setup-recommendations provided with the SYBR® Green I Master dye Kit (Roche).

The SYBR® Green I Master dye send out fluorescence light when bound to double-stranded DNA. Under denaturation of double stranded DNA the SYBR® Green is released causing drastic reduction in the fluorescence. During the polymerization, primers anneal starting the generation of newly synthesized PCR product. After the polymerization, more SYBR® Green I Master dye will be able to bind due to the amplification increasing the detectable fluorescence. Due to the molar excess of primers and thermostable DNA polymerase at the beginning, the DNA template will be the limiting substrate in the reaction making the fluorescence detection proportional to the amount of DNA template. After a certain amount of cycles, a threshold level is reached giving rise to a Cp value (crossing point/ crossing threshold) reflecting the amount of DNA template present in the samples. The earlier the threshold level is reached the lower will the Cp value be, indicating a higher amount of template to begin with. Primers used are listed in appendix 2.

2.1.8 Reverse Transcriptase-PCR

After converting mRNA to cDNA the quantity of RNA can be detected by PCR using suitable primers which can amplify the cDNA of interest. The amplified cDNA is then run on an agarose gel where the size and amounts of cDNA are estimated.

2.1.9 Gel electrophoresis

PCR samples were checked by agarose gel electrophoresis, which separates the DNA or RNA fragments according to size. Depending on the expected sizes of the fragments different percentages of a SeaKem® Agarose was used in 1 X TAE (Tris acetate, EDTA). Ethidium Bromide (EtBr) was added to the gel and the results were visualized under UV-light. The more fragments of a given size the stronger the band will appear when visualized giving an indication of the amounts of a given fragment. The gels were run on 85-100V for 30-60 minutes depending on the size of the gel. 6 X FBX loading dye (15 % Ficoll 400 (GE Helthcare), 0.25 % Orange G (Sigma), dH_2O) was added to the samples to a final concentration of 1 X FBX before loading the samples on the gel. For determination of the size the DNA standard 1Kb ladder (Thermo Scientific) was loaded on the gel.

2.1.10 Quantification of DNA and RNA

Quantification of DNA and RNA was done using the NanoDrop® 2000 UV-Vis Spectrophotometer (Thermo Scientific) or NanoDrop® ND-1000 UV-Vis Spectrophotometer (Thermo Scientific). The NanoDrop instrument calculates the DNA or RNA concentration based on the Beer-Lambert equation: $A = \varepsilon * b * c$ where A is the absorbance (RNA and DNA have A260), ε is the extinction coefficient ($L * mol^{-1} * cm^{-1}$), b is the length the UV travels in cm, and c is the concentration (moles/liter).

2.1.11 Sequencing

Sequencing was performed by the ABI laboratory at the *Department of Bioscience, Faculty of Mathematics and Natural Sciences, University of Oslo N-0316.*

2.1.12 Genotyping of SALK-lines

For genotyping mutant lines the REDExtract-N-Amp Plant PCR Kit (Promega-Aldrich). This kit allows rapid DNA extraction and PCR preparations. Extraction buffer was added to leaf discs from plants to be analyzed and incubated at 95 °C for 10 min before Dilution buffer was added. Extracted DNA was stored at 4 °C. PCR on extracted DNA was run using REDExtract-N-Amp™ PCR ReadyMix™ (Promega-Aldrich) and genotyping primers (appendix 2).

2.1.13 Gateway® cloning system by Invitrogen

The Gateway® cloning system is based on the site-specific recombination system of bacteriofag lambda (λ) enabling it to transfer DNA to the *Escherichia coli* genome (Landy, 1989). The site-specific *att*achment sites, *att* sites, allow insertion of a DNA sequence into a vector without altering the orientation and reading frame as the attB1 site only will recombine with attP1 and not attP2 and attL1 only will recombine with attR1. The recombination of these sites is mediated by the BP clonase™ enzyme which recombines attB sites the DNA sequence with attP sites in the vector resulting in entry clones with attL sites. An LR clonase™ enzyme recombine the attL sites with attR sites in the destination vector of your choice.

By using primers with flanking attB sites the promoter region of *LBD37, LBD38*, *LBD39* and *LBD41* with flanking attB sites were quantified. (Primer sequences used for quantification of LBD promoter regions with flanking *attB* sites are listed in appendix 2). The attB flanked PCR products were then recombined with the attP sites of the donor vector pDONR™/Zeo (Invitrogen) resulting in an entry clone and a by-product. The attL sites of the entry clone containing the promoter region were then recombined with attR sites in the destination vectors pMDC162 (section 2.1.15) and pHGY (RIKEN Plant Science Center) for the making of expression clones with the reporter gene β-Glucoronidase (GUS) and Fluorescent Protein (YFP), respectively (figure 2.1). The donor vector and the destination vectors had a *ccdB* gene as a negative selection marker that ensured the survival of *E. coli* cells containing the promoter region and not the *ccdB* gene, as the ccdB interferes with the DNA gyrase activity killing the *E. coli* cells. As a positive selection marker, the donor vector encoded a zeocin (zeo) resistance gene, while the destination vector pMDC162 encoded a kanamycin (Km)

resistance gene and pHGY encoded a Spectinomycin (Sp) resistance gene. The antibiotic resistance ensured the survival of the *E. coli* cells containing the vector of interest on plates with the respective antibiotic. The BP reaction and LR reaction were performed according to the manufacturer's recommendations. For termination of the BP and LR reaction, 1 µl Proteinase K (Invitrogen) was added as the enzyme degrades the reaction enzyme. Solutions were incubated at 37 °C for 10 min.

Correct insertion of the respective promoter regions was confirmed by sequencing using the same primers that was used for amplification of the LBD promoter regions (for primer sequences see appendix 2).

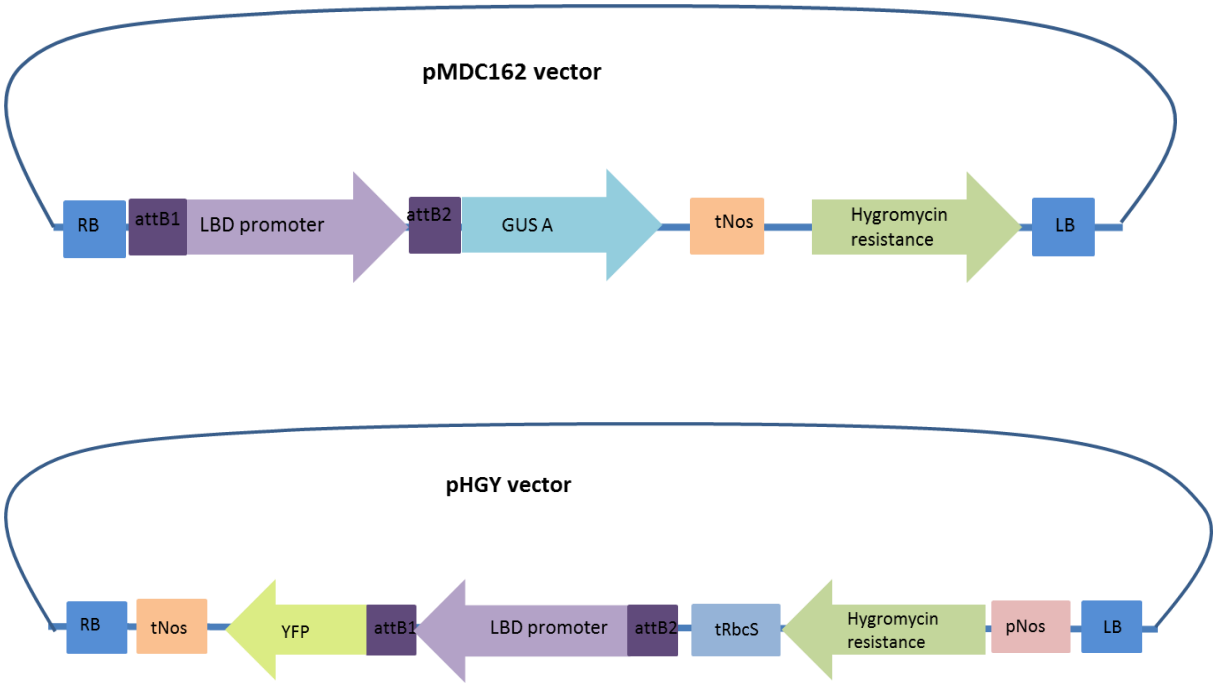

Figure 2.1: Illustration of the two LR vectors with the integration of the LBD promoter region upstream of the reference gene. Both vectors supply the infected plants with hygromycin resistance (green arrow) enabling easy selection of transformants.

2.1.14 Plasmid DNA purification of lysate

Plasmid DNA from *E. coli* was purified using the Wizard®Plus SV Minipreps DNA Purification System Kit (Promega) following the centrifugation protocol provided with the kit. After making bacterial lysate the cleared lysate was transferred to a column inserted into a collection tube followed by centrifuged. After discarding of flow-through the membrane in the column was washed twice with Wash solution previously diluted with EtOH. Plasmid DNA was eluted into a new sterile Eppendorf tube with nuclease-free water.

2.1.15 Midiprep Plasmid purification

For recovering a larger amount of plasmid DNA, a JetStar™ 2.0 Plasmid Kit-Midi (Genomed of Life Technologies Corporation) was used and the recommended protocol from the manufacturer was followed. The Midiprep was performed on bacteria pellet of bacteria with pMDC162 vector containing a Km resistance gene. The pellet was resuspended in resuspension solution, lysed with lysis solution followed by neutralization of the lysate by the addition of Neutralization solution. Supernatant was run through a previously equilibrated column by gravity flow. Column was the washed with Column wash solution. Plasmid DNA was eluted by addition of preheated DNA elution solution. Isopropanol was added to precipitate the plasmid and the pellet containing plasmid DNA was washed with 70 % EtOH. When totally free of EtOH the pellet was resuspended in MilliQ-water and stored at -20 °C.

2.2 Bacterial techniques

2.2.1 Bacterial growth conditions and selection

2.2.1.1 Growth and selection of *E.coli*

Optimal growth temperature for *E. coli* is 37 °C and *E. coli* has a generation time of about 25 min depending on the *E. coli* strain. Inoculation time was between 16-20 h before reaching the stationary phase. For selection, different antibiotics were used depending on the antibiotic resistance of the transformed *E. coli*. Transformed E. coli was always grown in liquid or on solid LB (10 g/l Peptone, 5 g/l Yeast extract, 10 g/l NaCl) media containing the respective antibiotics.

2.2.1.2 Growth and selection of *A. tumefaciens*

The optimal growth temperature for *A. tumefaciens* is 28 °C and has a generation time of about 1 h depending on the strain. Inoculation time was around 48 h before reaching stationary phase. For selection antibiotics, to which the *Agrobacteria* were resistant, as well as the antibiotic resistance provided by the plasmid DNA, was added to both the solid growth media and the liquid YEB media. (YEB = 5 g/l Beef extract, 1 g/l Yeast extract, 1 g/l Bacto Peptone, 5 g/l sucrose, pH set to 7,4 and after autoclavation addition of 2 ml 1 M MgSO4).

2.2.1.3 Freezing stock

Freezing stocks were made for all of the different transformed bacteria cultures: 50/50 of bacterial culture and 80 % Glucose solution was mixed before storing at - 80 °C.

2.2.2 *Escherichia coli* transformation by heat shock

E. coli transformation was performed by heat shock. 1 µl plasmid DNA was added to a one shot DH5α™ Chemically Competent cells (Invitrogen) or One Shot® Top10 Chemically competent cells (Invitrogen) and heat shocked at 42 °C for 40 sec, just enough to make the cell wall permeable for the surrounding plasmid DNA without killing the cell. After addition of SOC medium, the transformed *E. coli* cells were shaken at the optimal growth temperature, 37 °C, for 1 h before plating out on plates containing LB medium with the respective antibiotics. For *E.coli* with pDONRzeo vector zeo was added to a final concentration of 2.5 ng/µl. For the GUS constructs, using pMDC162 with Km resistance, Km were added to the growth media to a concentration of 100 ng/µl, while for the YFP constructs using pHGY vectors with Sp resistant, Sp were added to a concentration of 50 ng/µl.

2.2.3 *Agrobacterium tumefaciens* transformation by electroporation

For transformation of *A. tumefaciens* electroporation was used. Here the plasmid DNA was added to a one shot of electro competent C58 GV3101 or C58 GV2260 *Agrobacteria* cells. An electrical shock was applied to the reaction creating pores on the cell wall of the agrobacteria making it possible for the surrounding plasmid DNA to enter the cells. SOC medium was added after the electroshock and the cells were left shaking at 28 °C for 1-2 h to recover before plating out on previously made YEB plates containing the respective antibiotics; Km for GUS constructs and Sp for YFP constructs. In addition to the antibiotic resistance provided by the different constructs GV3101 *Agrobacteria* strain had Rifampicin (Rif), Gentamycin (Gent) and Km resistance while the GV2260 strain had Rif and Gent resistance. GV3101 was used for the YFP constructs while GV2260 was used for the GUS constructs. Km and Rif were added to a final concentration of 100 ng/µl, while Gent was added to a final concentration of 7 ng/µl.

2.2.4 Preparation of *Agrobacteria* solution for floral dipping

For floral dipping the transformed agrobacteria were cultured in a 500 ml Erlenmayer flask containing YEB medium and the respective antibiotics in a total volume of 250 ml. The cultures were inoculated shaking at 28 °C for about 48 h depending on how fast the agrobacteria was growing before measuring the OD. OD had to be no more than 1.2 before proceeding with the making of the infiltration culture keeping the bacteria in the stationary phase. If the OD_{600} ≥1.2 the bacterial culture was diluted to an OD lower than 1.2 and incubated until the OD reached 1.2 again. When OD ≤ 1.2 the cultures were centrifuged using a TJ-25 centrifuge (Beckman Coulter, Inc.) with a TS-5.1-500 rotor for 10 min at RT, 5000 rpm. Pellets were then dissolved in 5 % Sucrose solution until it reached OD_{600} = 0.8. Before the floral dipping, Silwet L-77 (Lehle Seeds) was added to a total of 0.02 %. This was to make the infiltration easier for the *Agrobacteria*.

2.2.5 Production of cleared bacteria lysate

For lysing the bacterial culture, the protocol for the Wizard®Plus SV Minipreps DNA Purification System Kit (Promega) was followed. The bacterial cultures were pelletized by centrifugation using a table centrifuge. The pellet was resuspended by using Cell Resuspention Solution. The bacteria cells were lysed by the addition of Cell Lysis Solution. Alkaline Protease solution was added to digest the proteins in the bacterial cell before the addition of neutralization solution. Cleared lysate for further purification of plasmid DNA was gained by centrifugation to separate the precipitated digested proteins from the plasmid DNA in the supernatant.

2.3 Plant techniques

2.3.1 Seed sterilization and growth conditions

Before plating out seeds they were sterilized to get rid of mold and bacteria that may follow the seeds. 70 % Ethanol was applied to the tubes containing the seeds and incubated at room temperature for 5 min. EtOH was poured off and Bleach solution containing 20 % Klorix in 0,1% Tween 20 and double-distilled H_2O (ddH_2O) was added. After 5 min, Bleach solution was poured off followed by addition of wash solution. Finally 0,1 % agar were added before pouring the seeds onto the MS-2 (Murashige & Skoog Medium, sucrose, KOH to set the pH to 6,3 and Bacto Agar) plates with or without antibiotics depending on whether the seeds were expected to have a resistance or not. Seeds were distributed on the plates by rotation. Plates were sealed off using surgical tape. The plants were placed in the growth room at 22°C under Long Day conditions with light intensity 100 µE/m2 after 1-2 days at 4 °C in the dark. After 10-14 days the seedlings were transferred to soil keeping the plants at 18 °C under Long Day conditions. For harvesting seeds older plants were placed in a harvesting room to dry before collecting the seeds.

2.3.2 Transformation of Arabidopsis thaliana

Col-0 plants for transformation were trimmed before transformation to get more branches for the floral dipping. When the plants had recovered from the cutting and gained more branches the plants were held upside down and dipped into the solution containing transformed *Agrobacterium tumefaciens* and Silwet L-77. After infecting the plants with the transformed *Agrobacteria*, the plants were laid down on wet paper towels in a tray and wrapped in aluminum foil O.N in the dark before transferring them back in the growth room for recovery and further growth.

2.3.3 Selection of GUS and YFP lines

After transformation seeds (T_1) from the transfected plants (T_0) were collected and plated out on plates containing the respective antibiotics (hyg in both cases). Plates with a 3:1 segregation of transformed: non-transformed plants was selected as these are hemizygous. To find homozygous lines in the T_3 generation seeds from the different hemizygous T_2 lines were plated out to find the plates with only transformed plants indicating homozygous lines.

2.3.4 Histochemical GUS analysis

Histochemical GUS analyses were performed on *proLBD::GUS* lines in wt, *ida* and *haehsl2* as well as *proKNAT::GUS* lines in *lbd38lbd39*. Seedlings and the floral positions 2, 4, 6, 8, 10, 12, 14 and 16 from the T1 and T2 generation were stained with the substrate 5-bromo-4-chloro-3-indolyl ß-D-glucuronide (X-Gluc). At 37 °C X-Gluc is cleaved by β-Glucoronidase into glucoronic acid and chloro-blomoindigo. When oxidized the chloro-blomoindigo dimerize giving a blue colored precipitate that is visible in regular light. Although the optimal temperature for GUS A is 37 °C the *proLBD::GUS* lines were incubated at RT due to the highly active promoters.

Before staining the different tissues were harvested into wells containing ice cold 90 % Acetone. The staining was done by incubation of the tissue in the staining buffer (5ml 500mM $NaPO_4$ pH7.2, 1 ml 100mM $K_4Fe(CN)_6$ x $3H_2O$, 1ml $K_3Fe(CN)_6$, 0,5 ml 10% Triton X-100, 42,5 ml dH_2O) containing 1ml 100mM X-gluc in dimethylformamide (DMF) for 0,5-20 h. After staining the tissues were dehydrated by incubation in a graded EtOH series to 70 % (15 % EtOH, 35 % EtOH and 50 % EtOH solutions were diluted with 50mM $NaPO_4$) before fixation with FAA solution (10 ml EtOH, 7 ml dH_2O, 2 ml Glacial Acetic Acid and 1 ml 37 % Formaldehyde). After fixation the tissues were rehydrated by incubating the tissues in a reversed graded EtOH series to 0 % EtOH.

The samples were mounted on microscopy slides covered with a few drops of clearing solution (8g Chloral hydrate, 2 ml dH2O and 1 ml 87 % Glycerol). The specimen was left to clear at 4 °C for at least 1 h before inspection.

2.3.5 petal breakstrength

Petal break strength (pBS) measurements is a method used to quantify the force in gram equivalents needed to separate a flower petal from a flower (Butenko et al., 2003). The petal breakstrength is measured using an instrument built after the petal breakstrength meter presented in Lease et. al. (2006). A few modifications were made; here a small ultrathin clamp was suspended from a force transducer (AD Instruments MLT050/D, range 0 - 50 g) by a nylon thread, thus improving the sensitivity of the pBS measurements. The force transducer converts the force needed to remove petals into volts using a Weatstone bridge circuit. A differential amplifier (Linear Technology LT1013) was included for linear amplification of the signal output from the force transducer. A 10-bit microcontroller (Microchip 12F675) was used to convert the transduced signal to a digital signal and communicate the data to a computer by converting the 10- bit value to a 4-byte ASCII packet. Another microcontroller (Microchip 16F676) was used to handle the Light-emitting diodes (LEDs) and the manual push button. The LEDs indicated when the force exceeded the maximum measureable strength and when the instrument was ready for a new measurement. The push button was pushed to prepare for a new measurement.

The petal breakstrength of two petals from each position, position 2, 4, 6 and 8 were measured and the numbers were compared to Col wt. Around 14-18 plants from each mutant line were measured from which a mean and standard deviation was calculated.

2.3.6 Crosses between different mutant lines and GUS and YFP lines

To make crosses the plant used as the mother was stripped of already pollinated flowers and buds that were too small to use in the crossing. The remaining 3-5 buds were emasculated, removing everything except the carpel, using a pair of tweezers previously cleansed with 70 % EtOH. To pollinate the mother carpel pollen from the father was drizzled onto the carpel. There were done crosses between *ida, haehsl2, knat2/knat6, proKNAT2::GUS, proKNAT6::GUS, proBP::GUS* and *lbd* double mutants, *lbd* single mutants, *proLBD::GUS* and *proLBD::YFP* lines.

2.4 Microscopy techniques

2.4.1 YFP lines

To investigate the YFP expression in the transfected plants, floral position 2-16 were investigated using an Axioplan2 Fluorescence Resonance Energy Transfer (FRET) Microscope (Zeiss) and a Leica M205 FA Fluorescence Stereomicroscope (Leica Microsystems) with UV-light excitation for visualization of YFP expression. YFP emits light at a wavelength around 525-530 nm. The different floral positions were taped onto a microscope slide using a two-sided tape. 10 x and 5 x magnification were used. The stereomicroscope was used to investigate the T3 generation of YFP plants. A GFP filter was used instead of an YFP filter as the stereomicroscope lacked YFP filter. The samples were exited with a laser at 488 nm and light range 502-538 nm was collected. Field of view (FOV) was set to be 4, 84 mm while depth of view (DOV) was 111 µm. Pictures were taken using a Leica DFC FX Monochrome digital camera (Leica Microsystems).

2.4.2 GUS lines

GUS expression in seedlings and siliques at different positions were investigated using an Axioplan2 Fluorescence Resonance Energy Transfer (FRET) Microscopy (Zeiss) under visible light using a 20 x, 10 x or 5 x magnification. The pictures were taken by an AxioCam HRc.

2.4.3 Pictures of *hae hsl2 lbd38 lbd39*

Pictures of the siliques along the inflorescence of the quadruple mutant *hae hsl2 lbd38 lbd39* were taken via a Nikon SMZ800 zoom stereomicroscope using a AxioCam ICr 1 (Zeiss) camera.

2.5 Bioinformatics

2.5.1 BLAST

Blast (http://blast.ncbi.nlm.nih.gov/Blast.cgi) was used to compare sequences and finding compatibility between sequencing results and the original sequence.

2.5.2 Vector NTI Advance® 11,5

Vector NTI Advance 11 (Invitrogen/www.lifetechnologies.com) was used for sequence analysis and for designing and ordering of primers as well as to create genetic maps over the different vectors. ContigExpress (Invitrogen) was used to look at sequencing results from the ABI lab, both the sequence and the chromatogram.

2.5.3 The Arabidopsis Information Resource

Arabidopsis.org is a database that provides genetic and molecular biology data for the model organism *Arabidopsis thaliana*. The Arabidopsis Information Resource (TAIR) was used to find gene sequences and promoter regions as well as to find information about different genes and publications on closely related subjects.

2.5.4 Alignments and making of Phylogenetic tree

For the making of phylogenetic tree and alignment of the class II LBD family members UniProt.org was visited. UniProt.org uses the ClustalO program.

2.6 Statistics

2.6.1 Calculation of relative expression

Relative expression of a target gene was calculated from Cp values given by the qPCR machine using Michael W. Pfaffl's (Pfaffl, 2001) model where E is the Real-Time PCR efficiency and the ΔCp is the deviation between mean Cp of control – mean Cp of sample. Both E and ΔCp are found for both the reference gene and the target gene. The relative expression ratio is then found by E target squared ΔCp target divided on E reference squared ΔCp reference as seen below.

$$R = \frac{E_{(target)}^{\Delta Cp_{(target)(control-sample)}}}{E_{(reference)}^{\Delta Cp_{(reference)(control-sample)}}}$$

The house keeping gene actin-2 and chlorophyll a/b binding protein (CAB) was used as reference genes and E was set to 2.

2.6.2 Chi-square test

Pearson's chi-square test was performed to check the goodness of fit by checking whether or not observed distribution differed from expected distribution. The chi-square test is defined as

$$X^2 = \sum_{i=1}^{n} \frac{(O_i - E_i)^2}{E_i}$$

where n equals the number of cells, O_i is the observed frequency, E_i is the expected frequency and X^2 is the test-statistics. Depending on the degrees of freedom and the critical value selected null hypothesis is either accepted or rejected depending on whether X^2 is lower or higher than the value given.

2.6.3 Standard deviation

Calculation of standard deviation was calculated using the equation below to check how large the range is between the numbers given by the same experiment. Standard deviation is defined as the squared root of variance which is the average of the squared differences between the different numbers and the mean of the numbers. When calculating variance of N values it is important to divide on N-1 when calculating variance.

Variance:

$$s^2 = \frac{1}{N-1}\sum_{i=1}^{N}(x_i - \bar{x})^2$$

Sample standard deviation:

$$S = \sqrt{\frac{1}{N-1}\sum_{i=1}^{N}(x_i - \overline{x})^2}$$

2.6.4 Student's T-test

The Student's T-test is used to determine whether two sets of data are significantly different from each other by testing the null hypothesis saying there is no difference. By using the t-test H_0 will either be accepted or rejected depending on the outcome of the t-test. Degrees of freedom were n-1 as two data sets were compared. Level of significance was set to 0, 05 providing a 95% probability of correctly rejecting or accepting the null hypothesis.

The formula is as follows

$$t = \frac{\overline{x} - \mu_0}{s/\sqrt{n}}$$

where $\bar{X}$ is the sample mean, μ_0 is the specified value, s is the standard deviation of the sample and n is the sample size.

Sets of data from pBS measurements of single mutants and double mutants, $\bar{X}$, were compared with pBS measurements of wt, μ_0. As these are individual sets of data unpaired T-test was performed and since the pBS of the single and double mutant could be both higher and lower compared to wt the t-test was two-tailed.

3 Results

The main goal of this thesis was to investigate the potential role of plant specific transcription factors from the LBD family in floral organ abscission by genetic analysis. Microarray data from Arabidopsis (unpublished data) suggests that LBDs may act downstream of IDA and HAE HSL2. So far there has been no genetic evidence of LBDs acting in IDA signaling pathway, thus the finding of elevated expression of *LBD37* and *LBD39* in *ida* and *haehsl2* (section 3.1) was the starting point for the investigation of LBD37 and LBD39 together with the two closely related LBDs, LBD38 and LBD41. To investigate the expression pattern of the four *LBD* genes in various tissues and their expression pattern during floral organ abscission GUS and YFP reporters were expressed under the promoter region of the *LBD* genes using the Gateway cloning systems as described in section 2.1.13 followed by transformation of Col wt by floral dipping as described in section 2.3.2. To investigate the role of the *LBD* genes in the regulation of floral organ abscission phenotypical investigations of floral abscission were performed for single and higher order T-DNA *lbd* mutant plants. Quantitative studies of the timing of floral abscission were recorded by pBS measurements. Further, we looked at the genetic interaction between the *LBD* genes and *IDA*, *HAE* and *HSL2*. LBDs regulate *KNOX* genes involved in meristem maintenance, *KNAT1*, *KNAT2* and *KNAT6* are three *KNOX* genes that later was also found to act in floral organ abscission. To elucidate any communalities between inflorescence development and floral organ abscission the possible relationship between LBD37, LBD38, LBD39 and LBD41 and KNOX proteins acting downstream of IDA was investigated by classic genetic studies including qRT-PCR analyses of *KNOX* expression in *lbd* mutant lines.

3.1 *LBD37* and *LBD39* are up-regulated in *ida* and *haehsl2* mutant lines

To confirm the microarray results (Liu et al., 2013) the expression levels of *LBD37* and *LBD39* were investigated in *ida* and *haehsl2* by qRT-PCR. RNA for cDNA synthesis was extracted from tissues from AZ at position 4 to 8 along the inflorescence.

Both *LBD37* and *LBD39* showed an up-regulation in *ida* and *haehsl2* mutant. *LBD37* was elevated to ~4 fold in *ida* and ~3 fold in *haehsl2*, while *LBD39* showed an up regulation to ~5 fold in *ida* and ~3 fold in *haehsl2* (figure 3.1) which suggested that IDA and HAE/HSL2 negatively regulates *LBD37* and *LBD39*. LBD38 and LBD41 are closely related to LBD37 and LBD39. Furthermore, *LBD38* and *LBD41* transcripts were found in open flower, floral buds and stems as well as in the inflorescence by RT-PCR (Shuai et al., 2002; Matsumura et al., 2009), thus *LBD38* and *LBD41* were included in the following investigations.

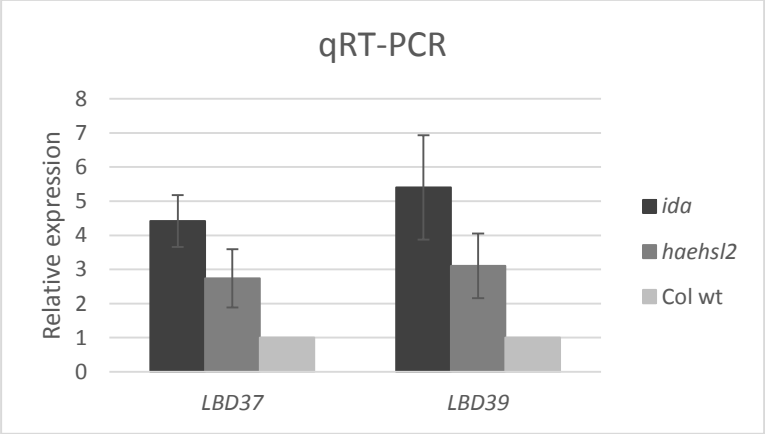

Figure 3.1: qRT-PCR analysis of LBD37 and LBD39 in i*da* and *haehsl2* mutant lines. Relative expression level of *LBD37* and *LBD39* in *ida* and *haehsl2* mutant compared to wt. Two biological and two technical replicas were used. (the expression level in wt was set to 1).

3.2 Expression pattern of *LBD37*, *LBD38*, *LBD39* and *LBD41*

To investigate the general expression pattern of the *LBD* genes fragments of 2535bp of the *LBD37* upstream region, 2564bp of the *LBD38* upstream region, 1991bp of the *LBD39* upstream region and 1988bp of the *LBD41* upstream region was amplified by PCR and cloned into the LR vectors pMDC162 and pHGY containing GUS and YFP reporter genes, respectively, as described in section 2.1.13. The reporter constructs were finally transformed into Agrobacteria before transformation of wt plants. Segregation between Hyg resistant and Hyg sensitive was scored and T-DNA insertions were predicted in the T2 generation for selection of single insertion lines and T3 for selection of homozygous lines. T2 generation of GUS reporter lines and T3 generation of YFP reporter lines were investigated for GUS and YFP expression in floral position 2-16 (first position is defined as the first flower with visible

white petals on top of the inflorescence (Bleecker and Patterson, 1997). GUS expression was additionally investigated in 12-day-old seedlings of the T2 generation.

3.2.1 *LBD37, LBD38, LBD39* and *LBD41* are highly expressed in the Abscission Zone of Floral Organs

To investigate the expression of *LBD37, LBD38, LBD39* and *LBD41* in floral AZs and to investigate the change in expression during the abscission process GUS assessed and YFP assessed *LBD* expression was examined in floral AZ along the main inflorescence from position 2-16. As the YFP expression was weak only positions with the highest expression was included (figure 3.2). (For all the YFP expression pictures see appendix 3.) Mainly the GUS expression pattern will be addressed. GUS staining of the different positions revealed expression in early positions, 2 and 4. There was a slight increase in GUS expression at position 6 and the expression peaked at position 8 and position 10, where floral organs are fully detached. The expression intensity of *proLBD37:GUS, proLBD38:GUS, proLBD39:GUS* and *proLBD41:GUS* stayed relatively strong throughout the following positions and GUS expression in all the reporter lines was detected as late as position 16, the last position investigated.

proLBD37:GUS and *proLBD38:GUS* showed a drastic increase in activity from position 6 to position 8. While *proLBD37:GUS* and *proLBD39:GUS* showed a peaks in expression at position 8 (figure 3.3 A and C), *proLBD38:GUS* and *proLBD41:GUS* expression peaks at position 10 (figure 3.3 B and D). *proLBD38:GUS* showed the strongest GUS expression of all *promoter:GUS* lines (figure 3.3 B). *proLBD37:GUS* showed the highest level of expression at position 6 compared to the other promoter reporter lines (figure 3.3 C).

proLBD37:GUS expression at position 8 and 10 was localized to the AZ cells (figure 3.4 A). The activities of the other *LBD* promoters were stronger in the vascular system. All the *LBDs* showed strong expression at the junction between the filament, sepals, petals and the floral receptacle. From position 8-10 and onwards the expression level were stable for all the promoter *LBD* reporter lines, until position 16 where the GUS expressions were weakened in various degree.

At earlier positions, position 2 and 4, GUS expression was visible in the veins of the floral petals when the GUS reaction was left to incubate for a longer period of time (approximately 3 hours longer than the other positions presented) (figure 3.3 A position 2).

Common to all the GUS lines driven by the respective *LBD* promoters is the expression of GUS in the vascular tissues of the floral receptacle and stem. YFP reporter lines displayed a similar expression pattern as the GUS reporter lines (figure 3.2), although the YFP expression was weak (appendix 3). The YFP assessed expression of *LBD39* gave the strongest expression; while YFP assessed *LBD38* expression gave the weakest. *proLBD41:YFP* lines displayed a peak at position 12, two positions later than that in *proLBD41:GUS* lines, The expression of *LBD41* might be more internal, thus more difficult to detect with YFP.

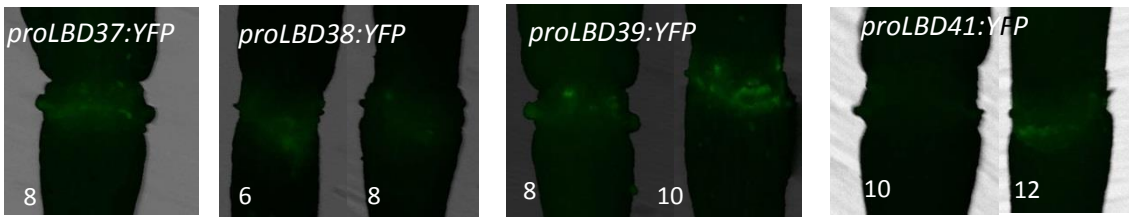

Figure 3.2: YFP assessed expression of the LBDs at positions with strongest expression.

YFP assessed LBD expression were weak in all the reporter lines and at all the positions.
A peak in YFP expression was still detected:
proLBD37:YFP peaked at position 8
proLBD38:YFP had a similar strength in expression from position 6-10
proLBD39:YFP showed the strongest expression and the YFP expression peaked around position 8-10.
proLBD41:YFP showed a strong expression at position 12.

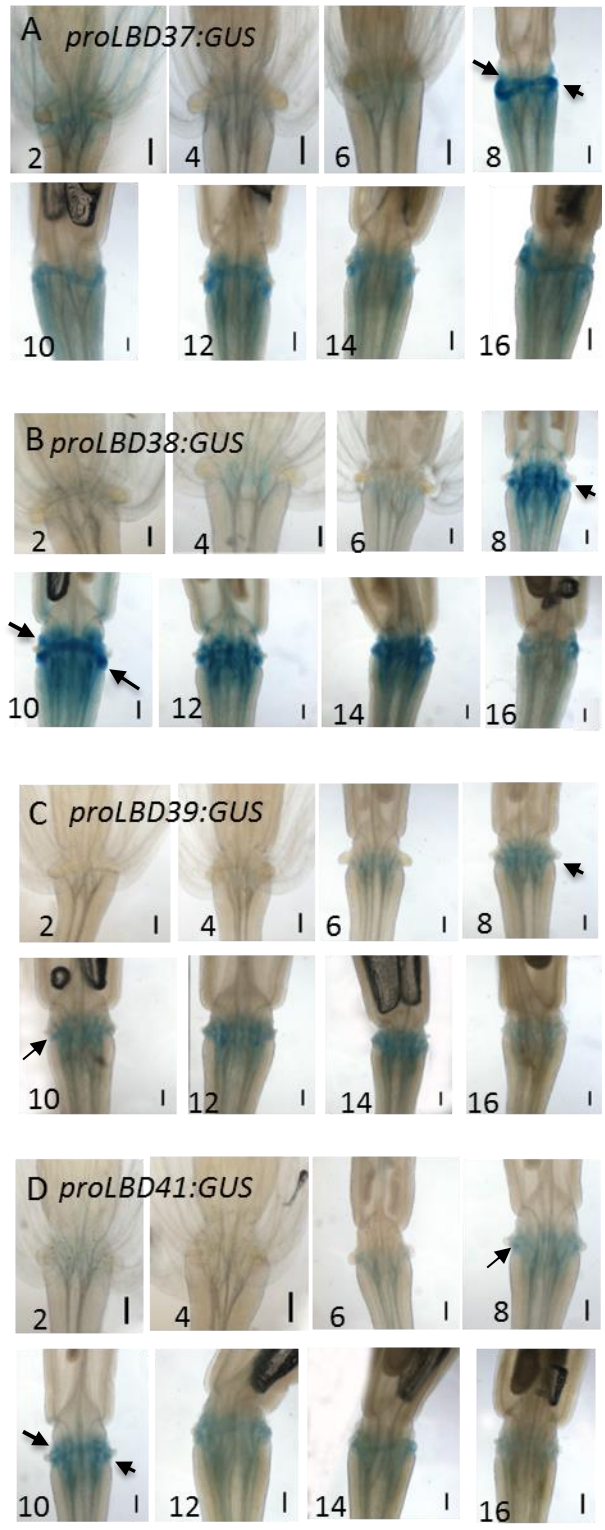

Figure 3.3 Expression pattern of the *LBD* genes in the AZ of position 2-16

A) *proLBD37: GUS* expression in AZs of different positions from position 2- 16 in Col wt

B) *proLBD38:GUS* expression in AZs of different positions from position 2- 16 in Col wt

C) *proLBD39:GUS* expression in AZs of different positions from position 2- 16 in Col wt

D) *proLBD41:GUS* expression in AZs of different positions from position 2- 16 in Col wt

(arrows indicate the expression at the floral AZ where expression was strongest) (Scale bars = 50 µm)
(the numbers in the lower left corners correspond to the positions on the inflorescence where position 1 is the flower at anthesis)

3.2.2 *LBD37*, *LBD38*, *LBD39* and *LBD41* are expressed in various tissues

Staining of 12-day-old seedlings revealed active LBD promoters in shot apical meristem (SAM), roots and the veins of cotyledons and young rosette leaves. When the GUS reaction was left to stain O.N *proLBD37:GUS, proLBD38:GUS* and *proLBD39:GUS* revealed expression in the endosperm layer of the mature seed after germination, possibly indicating a role in endosperm rupture during germination (figure 3.3 H). The expression of *proLBD37:GUS* was significantly higher than that of *proLBD38:GUS* and *proLBD39:GUS, proLBD39:GUS* having the weakest staining (appendix 5).

In roots the expression of the *LBD* genes in question was centered at the base of emerging lateral roots and in the layers endodermis, pericycle, phloem and xylem constituting the stele of the root (figure 3.4 C, D and E). Expression was also detected at the columella root cap and lateral root cap of the main and LR tip in the *proLBD37:GUS* , *proLBD39:GUS* and *proLBD41:GUS* lines. The *proLBD38:GUS* lines, on the other hand, only showed GUS expression in the LR tip (supplemental figure 3, appendix 5). Furthermore, the activity of *proLBD37:GUS* and *proLBD38:GUS* in the LR tip seems to increase with age as the younger LRs do not show any GUS expression while the older have a quite strong GUS expression. *proLBD41:GUS* line displayed overall the broadest expression pattern in roots with expression in the entire stele of the main root and LRs. *proLBD41:GUS* expression could also be seen in the epidermis and in the cortex, though the expression in the cortex was very weak (appendix 5). Both *proLBD38:GUS* and *proLBD39:GUS* lines showed GUS expression in the meristem zone, though not stretching past the apical region, while *proLBD37:GUS* did not show any GUS expression in the stele past the area of elongation (figure 3.4 D, E).

In the veins of cotyledons and young rosette leaves, all of the *promoter:GUS* constructs showed active *LBD* promoters (Figure 3.4 A and G). All the reporter lines with the exception of *proLBD37::GUS* (appendix 5) also showed expression in the hydratodes (figure 3.4 A and G), the secretory tissues from which water is secreted through pores in the margins of the leaves (Martin et al., 2000). All the reporter lines showed expression in the SAM (figure 3.4 B).

When staining the different positions expression was seen in the filament in proximity to the anther, in the style of the pistal and the veins of the floral petals. The *proLB41:GUS* had the

weakest expression in both stamen and style, while *proLBD39:GUS* lines showed the highest expression in the same tissues (figure 3.4 F). Many *LBDs* including *LBD37*, *LBD38*, *LBD39* and *LBD41* are found to be expressed in various tissues such as 12-day-old shoot tissue, rosette leaves, cauline leaves, inflorescence stem, root, floral bud and open flowers (Shuai et al., 2002; Matsumura et al., 2009).The finding of *LBD37*, *LBD38*, *LBD39* and *LBD41* promoters being active in in the various tissues further demonstrates their broad expression pattern.

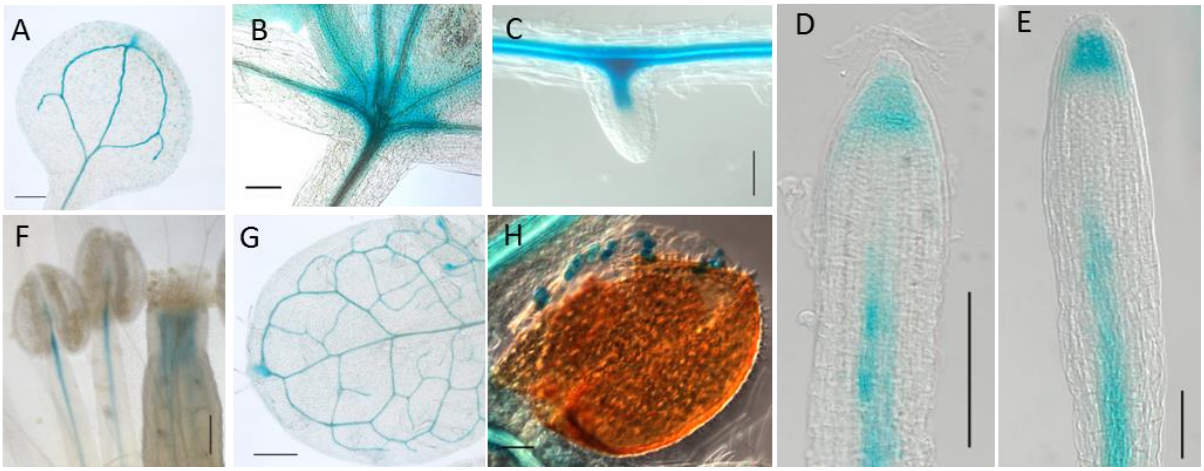

Figure 3.4 GUS assessed LBD expression in 12-day-old seedlings and full-grown plants.
(A) and **(G)** *proLBD41:GUS* expression in the veins of cotyledons and young rosette leaves and in the hydratodes. GUS expression in the vascular tissue of seedlings were detected in all the reporter lines, and GUS expression in the hydratodes were also seen in *proLBD38:GUS* and *proLBD39:GUS* lines.
(B) LBD expression in the SAM, here represented by *proLBD39:GUS.*
(C) to **(E)** Expression in the stele of LRs and main root and expression in the root cap of the main root tip and LR tips represented by *proLBD38:GUS* (C) and *proLBD37:GUS* (D, E).
(F) Expression of the LBDs in the style and stamen of flowers at position 2 and 4 are here represented by *proLBD39:GUS.*
(H) Expression of *LBD37*, *LBD38* and *LBD39* in the endosperm represented by *proLBD37:GUS* (Scale bars = A, B, C, D, E, G, H: 100 µM; F: 200 µM)

3.3 Investigation of LBD homozygous lines

3.3.1 Characterization of *lbd* mutants

Homozygous mutant lines *lbd37-1* (SALK_057939), *lbd38-2* (SALK_201956C), *lbd39-1* (SALK_011706) and *lbd41-2* (SALK_144556C) (appendix 4) were provided by The SALK Institute Genomic Analysis Laboratory (SIGnAL). All the mutant lines had the T-DNA inserted into the second exon with the exception of *LBD37* which likely had the T-DNA inserted into the 3´untranslated region (UTR). The expression level of the different LBDs in the respective mutant lines was investigated using Real-Time PCR (RT-PCR). mRNA for cDNA synthesis was extracted from siliques from position 4, 6 and 8 on the inflorescence of the four single mutant lines and Actin-2 was used as a reference gene. Actin-2 primers were used on the genomic DNA control as well as the genomic size of Actin-2 (~350 bp) is distinguishable from that of cDNA (~260 bp) (figure 3.6). Primers used to quantify LBD expression are listed in appendix 2. *lbd37-1* displayed a similar LBD37 level compared to that of wt (figure 3.6). As it turned out that *LBD37-1* had the T-DNA inserted into the 3´UTR region instead of in the exon as listed, this result was as expected. The expression level of *LBD38, LBD39* and *LBD41* in their respective mutant lines was not detectable. The lack of *LBD38, LBD39* and *LBD41* expression in the respective mutant lines (figure 3.5) indicate knockout of the LBD genes by the T-DNA insertion confirming that these lines are homozygous mutant lines. As *lbd37-1* was not a knockout allele, only double mutants of *lbd38-2*, *lbd39-1* and *lbd41-2* were further investigated.

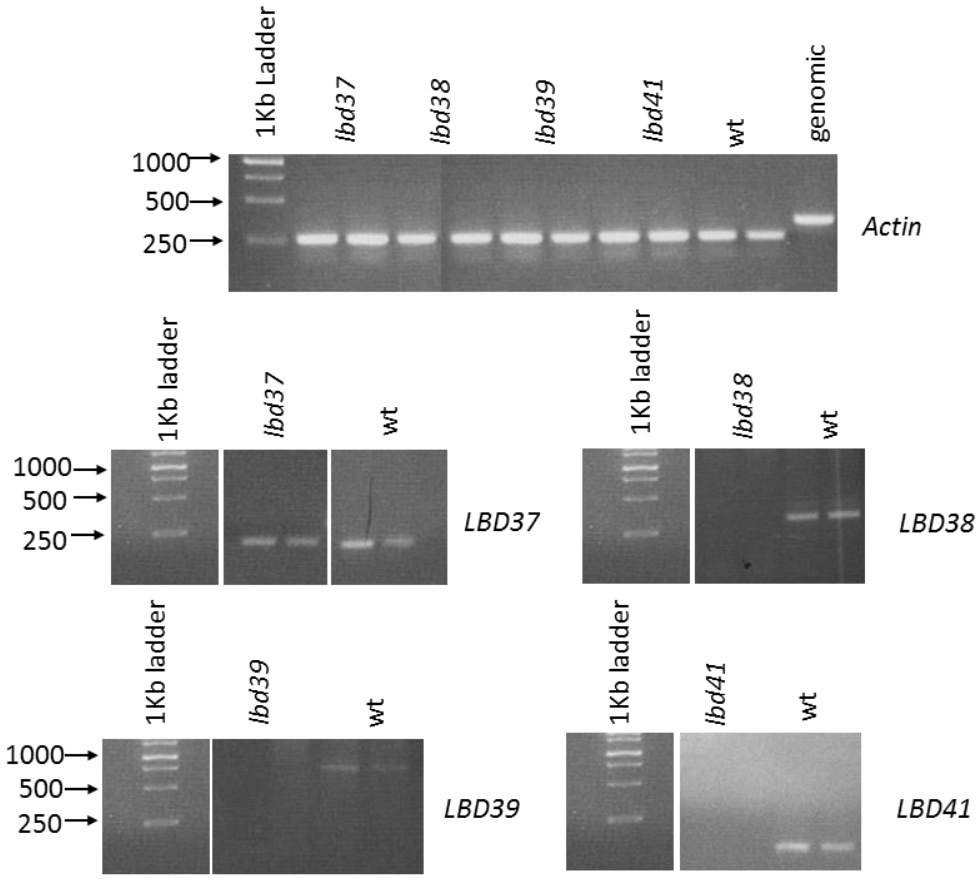

Figure 3.5: RT-PCR results of *lbd* single mutants.
For each plant line (mutant lines and wt) there were two genomic replicas both tested with actin-2 as well as the respective primers for the mutant lines (appendix 2). Only the *LBD37* expression level was seemingly unchanged in the mutant lines compared to wt. Expected band size was for *LBD37*, *LBD38*, *LBD39* and *LBD41* were 184 bp, 377 bp, 743 bp and 141 bp, respectively.

3.3.2 Abscission in *lbd* single mutants

To investigate the potential effect of loss of function of *LBD* genes on abscission, petal breakstrength of floral petals in early positions of *lbd* mutants were measured as described in section 2.3.5. The pBS profile of the single mutants was compared to the pBS profile of col wt (figure 3.6). The pBS profile of the *lbd37-1* single mutants did overall not show any significant difference in break strength compared to wt. With an expression level of *LBD37* in *lbd37-1* mutant line similar to that of wt it is not surprising to find the pBS profile of *lbd37-1* to be closest to the wt pBS profile. However, at position 4 *lbd37-1* line displayed a significant

reduction in pBS at a 95% confidence level with a P = 0.02. In contrast, *lbd38-2* mutant line showed a significant reduction in breakstrength at all the positions measured; position 2 (P = 0.004), 4 (P = 0.008) and 6 (P = 0.003) compared to wt. Single mutant lines of *lbd39-1* and *lbd41-2* also showed a significant reduction in petal break strength, though only at position 6 where *lbd39-1* showed the highest significant difference (*lbd39-1*: P = 0.0005 and *lbd41*: P = 0.004). This is in line with *proLBD39:GUS* displaying a higher expression at position 6 compared to the other *promoter:GUS* lines. Despite the significant differences, there was an overall minimal difference in pBS between the single mutants and wt as would be expected of factors acting redundantly. However, loss of *LBD38* had the largest effect on abscission by causing a reduction in petal breakstrength at all positions measured, while loss of *LBD39* had the largest impact on abscission at position 6 causing earlier abscission.

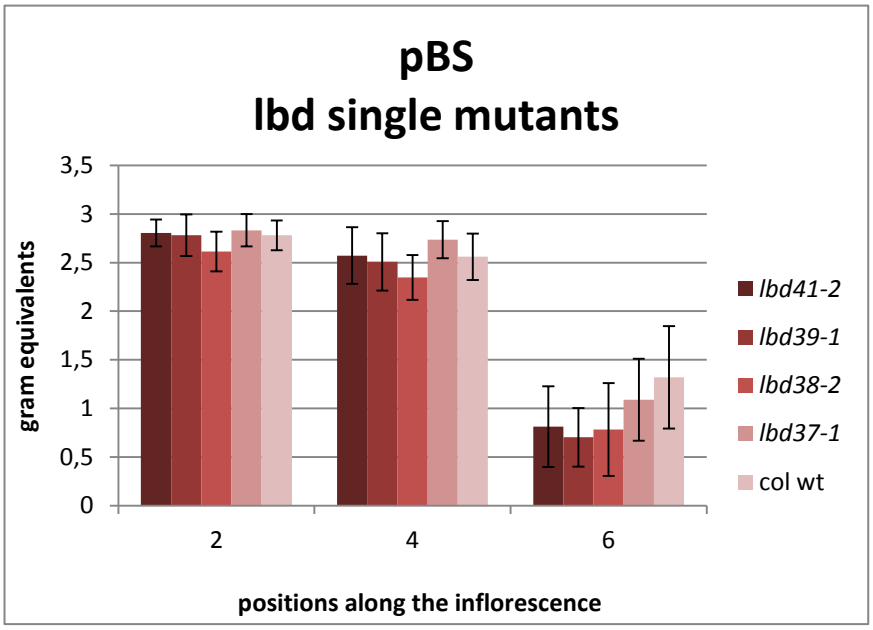

Figure 3.6: pBS profile of the single mutant lines compared to Col wild type.

(pBS = the force needed for the removal of flower petals given in gram equivalence)

(Bars= SD) (n = minimum 13)

3.3.3 *lbd41 lbd39*, *lbd38 lbd39* and *lbd41 lbd38* show early floral organ abscission

As LBDs are suggested to act redundantly and an increasing number of LBDs have been shown to be able to form complexes *lbd41-2 lbd39-1*, *lbd38-2 lbd39-1* and *lbd41-2 lbd38-2* double mutants were created. To confirm homozygous for the crosses genotyping was done as described in section 2.1.12. Homozygous lines were investigated for potential premature loss floral organs by pBS as described in section 2.3.5.

Compared to the pBS profile of the single mutants, the individual double mutant lines constituted pBS profiles displaying a higher reduction in petal breakstrength. *lbd41-2 lbd38-2* displayed the highest gram equivalence at all positions with a significant reduction only at position 6 (P = 0,006). *lbd38-2 lbd39-1* and *lbd41-2 lbd39-1* displayed a significant reduction at both position 4 (P = 0.001; P = 0.0002, respectively) and position 6 ($P = 2.16 \times 10^{-6}$; $P = 1.9 \times 10^{-7}$, respectively). The strong reduction in pBS seen in the double mutants *lbd41-2 lbd39-1* and *lbd38-2 lbd39-1*, especially at position 6, indicating early abscission and suggests earlier dissolution of the middle lamella between the floral organs and the floral AZ.

The double mutants *lbd38-2 lbd39-1* and *lbd41-2 lbd39-1* abscise organs at one position earlier than col wt (figure 3.7) as would be expected of transcription factors acting as suppressors during abscission activation. Since the pBS measured at position 2 of *lbd38-2 lbd39-1* and *lbd41-2 lbd39-1* was similar to wt and the reduction in pBS at position 4 compared to wt was low compared to the strong reduction in pBS at position 6, LBDs may be most active in inhibiting abscission at a time where cell wall loosening are initiated. As the LBD39 promoter showed most active at position 6, and as the *lbd39-1* mutant displayed a significant reduction in pBS at position 6 *lbd39-1* seems to have the strongest effect on floral organ abscission of the LBDs tested, and give an even stronger reduction of petal breakstrength in combination with loss of *LBD38* or *LBD41*. This supports redundancy between these LBDs and suggests formation of various regulatory complexes.

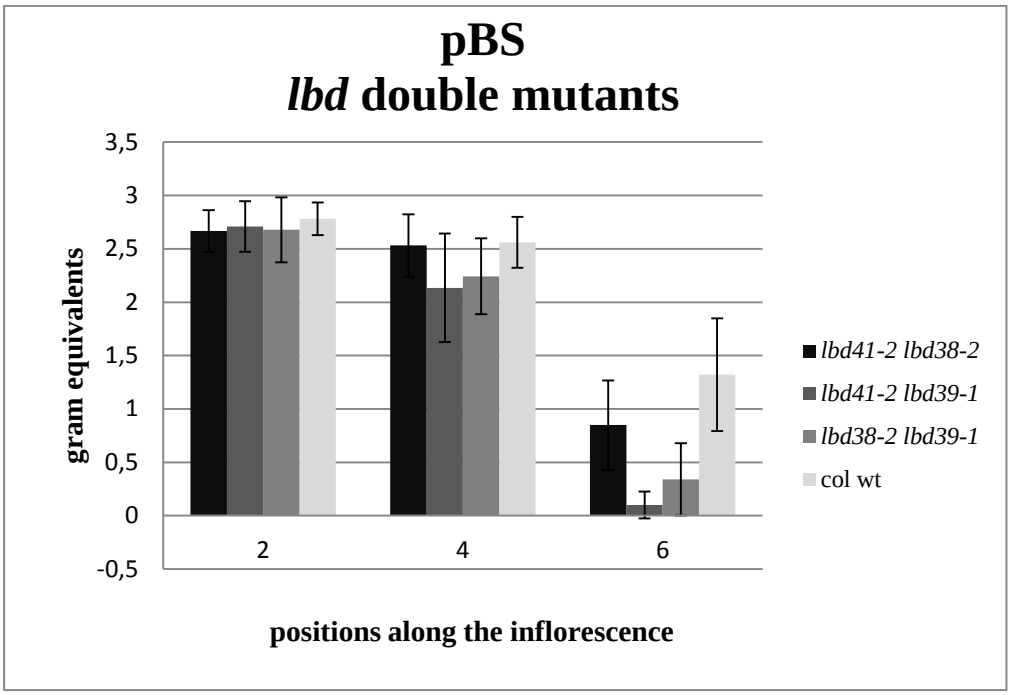

Figure 3.7: pBS of *lbd* double mutant lines compared to wt. Two petals were measured at each position measured (2,4 and 6). (pBS = the force needed for the removal of flower petals given in gram equivalence) (Bars = SD) (n = minimum 13)

3.4 Interaction between LBD and components of IDA signaling pathway

3.4.1 *LBD* expression in *ida-2* and *haehsl2* mutants

As the expression level of the *LBD37* and *LBD39* showed an increase in *ida* and *haehsl2* mutant lines *proLBD:GUS* lines were crossed to *ida* and *hae hsl2*. Due to time limitation *proLBD38:GUS* and *proLBD39:GUS* expression in *ida* mutant and *proLBD39:GUS* expression in *haehsl2* mutant were investigated.

proLBD38::GUS in *ida-2* mutant and *proLBD39::GUS* in *hae hsl2* double mutant did not show any expression (figure 3.8 D). However *proLBD39::GUS* in *ida* showed a very weak expression when stained for approximately 22 hours (figure 3.8 A to C). Since qRT-PCR results showed an upregulation of *LBD39* in *ida* and *haehsl2* mutant lines the lack of expression might be due to silencing of the already higly expressed *LBDs*. To verify possible silencing seedlings of the three constructs were GUS stained. As *IDA* is not expressed in the vascular tissue of the root like the LBDs, staining of the root will indicate whether the *LBD* promoter is active. Interrestingly the *proLBD38:GUS* expression in *ida* mutant showed high expression in the roots (figure 3.8 E, F), as in wt, although there was no expression in the meristem zone of the main root (figure 3.8 G) as seen in wt. There was high *proLBD38:GUS* expression in the hypocotyl-root junction in *ida* mutant (figure 3.8 E) as seen in wt (not shown). *proLBD39:GUS* expression in *ida* was weak in the entire seedling when compared to wt and lacked expression in the meristem zone of the root like *proLBD38:GUS* in *ida* mutant (figure 3.8 H, I). However, *proLBD39:GUS* showed expression in the main root tip of *ida* as seen in wt (figure 3.8 H). The promoter *LBD39* activity in SAM of *ida* mutants and especially the activity of *LBD38* promoter in SAM was very weak and there was no detectable GUS expression in the veins of young rosette leaves. However, in pro*LBD39:GUS ida* there was GUS expression in the veins of cotyledons. These results suggests that *LBD38* and *LBD39* are positively regulated by IDA, and not negatively regulated as the qRT-PCR results indicated. The reason for the up-regulation of *LBD* in *ida* detected by qRT-PCR results could be due to too low specificity of the qRT-PCR primers, a common problem with qRT-PCR.

The expression pattern of *HAE* and *HSL2* are broader in roots than that of *IDA*, and *HSL2* are like the *LBDs* expressed in the vasculature. In *hae hsl2* mutant the activity of the *LBD39*

promoter was undetectable (figure 3.8 D, J). As the HAE and HSL2 have overlapping expression pattern to the *LBDs*, the absence of GUS in *proLBD39:GUS hae hsl2* mutants could be explained if HAE/HSL2 positively regulated *LBD39*. However, the elevated *LBD39* expression level in *hae hsl2* mutant detected by qRT-PCR suggested HAE HSL2 to negatively regulate *LBD39* contradicting the results presented here, but this could also be due to low specificity of the primers as the same qRT-PCR primers were used. However, there is a possibility of total silencing of the *LBD39* promoter.

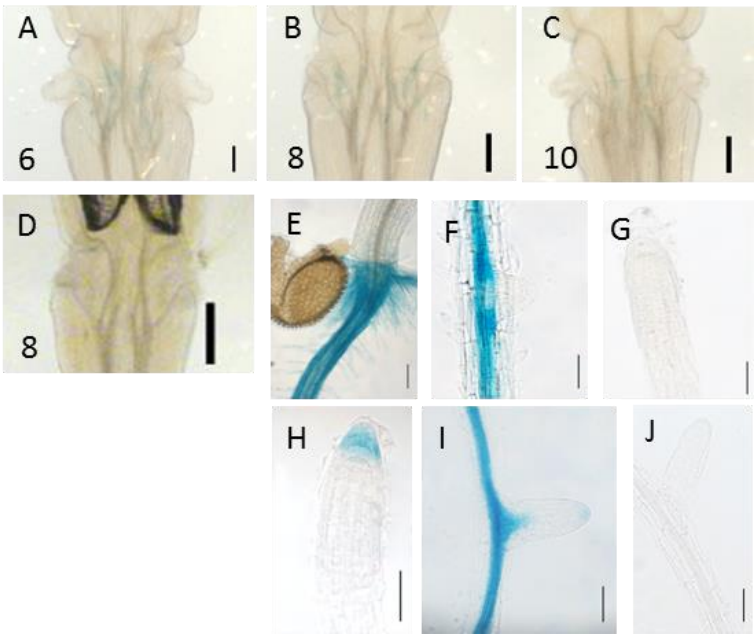

Figure 3.8: *proLBD38:GUS* and pro*LBD39:GUS* expression in the floral AZ and roots of *ida* and *hae hsl2.*
(A) to **(C)** Weak GUS expression in detected in the ventricular system in the AZ region of *proLBD39GUS ida-2* mutant at position 6, 8 and 10.
(D) No GUS expression in any of the positions investigated along the main inflorescence of neither the mutant lines *proLBD38GUS ida-2* nor *proLBD39 hae hsl2*. Lack of GUS staining is represented by *proLBD38GUS ida-2* position 8. (numbers at the lower left corner= positions along the inflorescence)
(E) to **(G)** *proLBD38:GUS* expression in roots of *ida* mutant.
(H) and **(I)** *proLBD39:GUS* expression in the main root cap(H) and in the emerged lateral root(I).
(J) No detectable GUS expression in the roots of *proLBD39:GUS haehsl2*.
(Scale bars = 50 μM)

3.4.2 Elevated *KNAT1* and *KNAT6* expression in *lbd* single mutants

LBDs, such as AS2 and JLO had the ability to suppress various *KNOX* genes in leaf development and during meristem patterning (Xu et al., 2003; Borghi et al., 2007; Iwakawa et al., 2007; Guo et al., 2008; Rast and Simon, 2012; Lodha et al., 2013). The same *KNOX* genes that are repressed by AS2 and JLO were found to be involved in floral organ abscission as well (Shi et al., 2011). For this reason, the potential regulatory effects of LBD37, LBD38, LBD39 and LBD41 on *KNAT1*, *KNAT2* and *KNAT6* were investigated. The mRNA, from which cDNA was made, was extracted from floral positions 4-8 from each single mutant line as described in section 2.1.3. The expression levels of the three *KNOX* genes in the *lbd* single mutants were measured by qRT-PCR using the comparative C_p method where two biological and three technical replicas were used.

As demonstrated in figure 3.9 there was an elevation of *KNOX* gene expression in *lbd37-1*, *lbd38-2*, *lbd39-1* and *lbd41-2* mutants compared to wt (wt expression was set to 1). In *lbd39* mutant line and *lbd37-1* mutant line the *KNAT1* expression level was elevated by a 2.6 fold and 2.4 fold respectively. *KNAT6* expression was elevated by a 3.5 fold in *lbd39-1* and a 3.2 fold in *lbd37-1* respectively. *KNAT6* was also up regulated in the other *lbd* mutant lines, though not as high; a 2.6 fold up regulation in *lbd38* mutant and a 2.4 fold up regulation in *lbd4-2* mutant. *KNAT2* expression was elevated by a 1.9 fold in *lbd37-1*, and 1.7 fold in *lbd38-2*, and 1.7 fold in *lbd39-1* and a 1.3 fold in *lbd41-2*, demonstrating an expression level closer to wt. The gene expression of *KNAT1* in *lbd38-2* and *lbd41-2* displayed an expression level close to wt as well with a 1.8 fold up-regulation in *lbd38-2* and a 1.9 fold up regulation in *lbd41*.

Taken together loss of LBD activities seems to have a larger effect on *KNAT6* expression than the other two *KNOX* genes tested and *KNAT1* expression was only up regulated in *lbd37* and *lbd39* mutants.

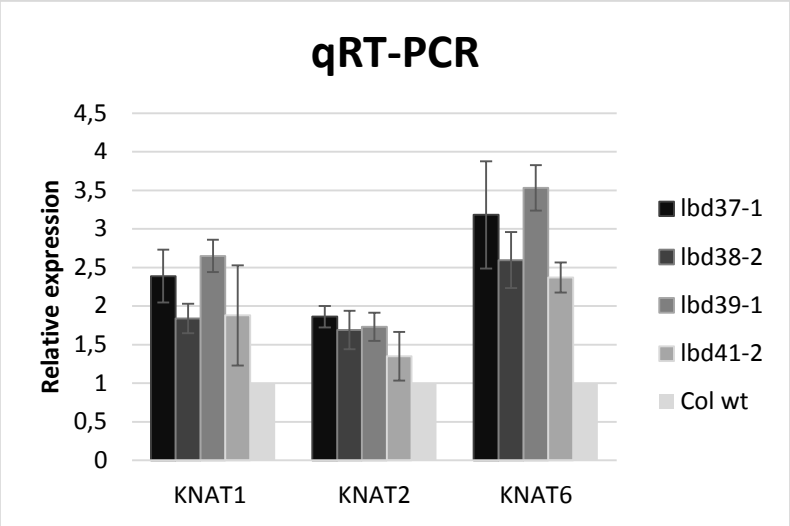

Figure 3.9: qRT-PCR analysis of *KNAT1*, *KNAT2* and *KNAT6* gene transcripts in *lbd37-1*, *lbd38-2*, *lbd39-1* and *lbd41-2* single mutant lines.
Relative expression level of the KNOX genes *KNAT1*, *KNAT2* and *KNAT6* in the *lbd* mutant lines compared to wt. Two biological and three technical replicas were used. (The expression level in wt was set to 1.)

3.4.3 Expression of *KNAT1* and *KNAT6* in *lbd* double mutants

KNAT1 is proposed to prevent premature abscission by restricting activation of CWR enzymes involved in cell separation through negative regulation of *KNAT2* and *KNAT6* (Shi et al., 2011). According to the hypothesis presented here, LBDs act as negative regulators of abscission by negatively regulating *KNAT2* and *KNAT6*. As the pBS results indicated a role of LBD39 in combination with either LBD38 or LBD41 in floral organ abscission as negative regulators, the possibility of LBDs negatively regulating *KNAT2* and *KNAT6* was investigated by expression analyses. To elucidate any connection between the LBDs and KNAT1, KNAT1 was also included. Due to limited time only *KNAT1* and *KNAT6* expression in *lbd38 lbd39* double mutant were investigated.

In comparison to the *proKNAT1:GUS* expression in wt *proKNAT1:GUS* expression in the *lbd38 lbd39* mutant showed significantly elevated GUS expression at all the position 2-8 with

a strong peak in GUS expression at position 8 (figure 3.10). However, the expression level at position 10 was in the double mutant lower at the AZ region compared to that in wt. In addition the *proKNAT1:GUS* expression is in the double mutant no longer restricted to the AZ, but was spread down along the pedicel. As the *KNAT1* expression level was elevated in the *lbd39* mutant, increased GUS assessed *KNAT1* expression in the double mutant was not surprising to find, however, the elevated GUS expression does not fit with the hypothesis of the LBDs only restricting KNAT2 and KNAT6 expression.

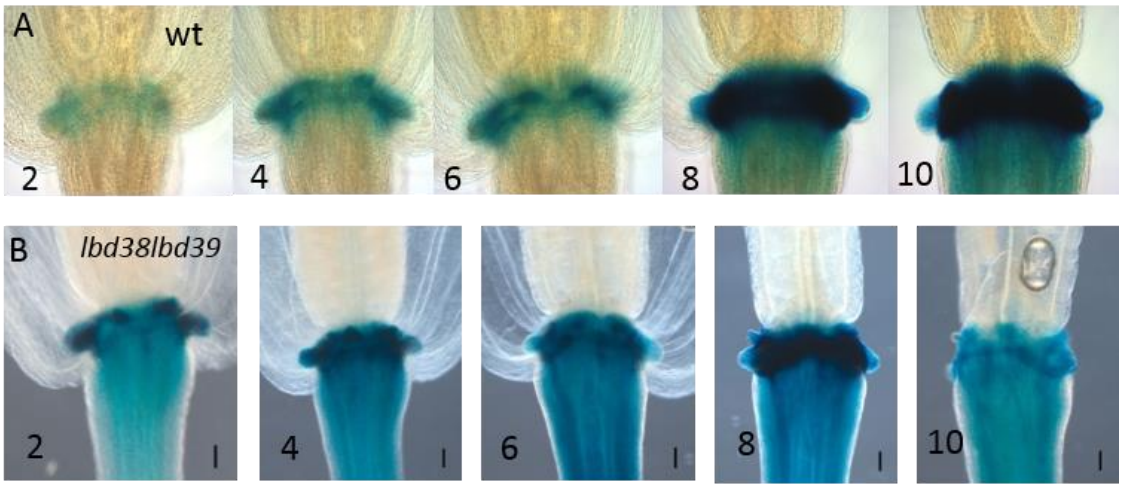

Figure 3.10: *proKNAT1:GUS* expression in the AZ of positions along the inflorescence of *lbd38 lbd39* mutant and wt.
(A) GUS assessed *KNAT1* expression in wt.
(B) *KNAT1* expression in the AZ of siliques along the inflorescence of *lbd38 lbd39* double mutant.
(Scale bars = 50 μM) (numbers at lower left corner = positions along the inflorescence)

Consistent with the hypothesis the expression level of *KNAT6* was highly upregulated in all the *lbd* single mutants compared to *KNAT1* and *KNAT2*. The expression pattern of *proKNAT6* in the *lbd38 lbd39* double mutant would then also be expected to be elevated. Compared to *proKNAT6:GUS* expression in wt the *proKNAT6:GUS* expression in *lbd38 lbd39* was elevated in position 2 and 4, while in position 6 - 10 the GUS expression was reduced (figure 3.11). Consistent with the hypothesis *proKNAT6:GUS* expression was elevated in early positions in the *lbd38-2 lbd39-1* double mutant, however the expression was lower in the following positions.

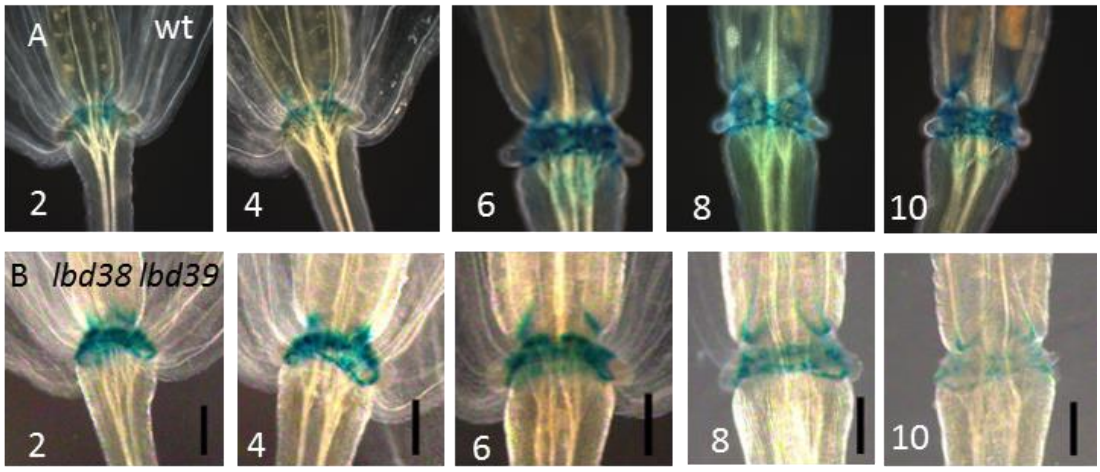

Figure 3.11: *proKNAT6:GUS* expression in AZ of floral position 2-16 along the main inflorescence of *lbd38 lbd39* mutant and wt.
(A) *proKNAT6:GUS* expression in wt.
(B) *proKNAT6:GUS* expression in the AZ of siliques along the inflorescence of *lbd38 lbd39* double mutant. (Scale bars = 50 μM)
(numbers at lower left corner = positions along the inflorescence)

3.4.4 *hae hsl2 lbd38 lbd39* quadruple mutant

Since *lbd39* showed an up regulation in *ida* and *haehsl2* and since *lbd39* single mutant displays early petal loosening at position 6 which increases with further loss of *LBD38* and *LBD41 lbd38 lbd39* and *lbd41 lbd39* were crossed to the *ida* and *haehsl2* mutant. As IDA need to bind HAE HSL2 in order to signal for abscission, crosses to *hae hsl2* will probably give a strong indication on whether LBDs act downstream of IDA-HAE HSL2. The *ida-2* mutant to which double mutants were crossed cannot be quantified by pBS, this as well as limited time lead to the investigation of two *haehsl2 lbd38 lbd39* mutant plants.

As not enough quadruple mutants were found to be able to make a reliable pBS profile in time, the pBS results will be presented in appendix 6 only to aid in the description of the phenotypical traits of the two quadruple mutants. In figure 3.13 position 6 and 8 in addition to a mature silique of the quadruple mutant have been photographed and compared to siliques of *hae hal2* mutant. Like in the *hae hsl2* the floral organs of *hae hsl2 lbd38 lbd39* fail to abscise (figure 3.12 C), thus additional loss of *LBD38* and *LBD39* are not able to fully rescue the phenotype of *hae hsl2*. However, at position 6 and 8 the floral organs of the quadruple mutant do not cling to the carpel as nicely as the floral organs of *hae hsl2* (figure 3.12 A, B), suggesting that the floral organs of *hae hsl2 lbd38 lbd39* may not be as strongly attached to the floral AZ as the floral organs of *hae hsl2*. This fits with the preliminary pBS results presented in appendix 6 that shows a strong reduction in pBS in *hae hsl2 lbd38 lbd39* at position 6 compared to that in *hae hsl2*. These findings allow us to speculate whether loss of *LBD38* and *LBD39* can cause loosening of floral organs along the main inflorescence of the *hae hsl2* mutants.

Figure 3.12: Pictures of different positions along the main inflorescence of the *hae hsl2* mutant and *hae hsl2 lbd38 lbd39* mutant.
(A) position 6 of *hae hsl2* (to the left) and *hae hsl2 lbd38 lbd39* (to the right).
(B) position 7 of *hae hsl2* (to the left) and position 8 of *hae hsl2 lbd38 lbd39* (to the right).
(C) mature silique from *hae hsl2* (to the left) and *hae hsl2 lbd38 lbd39* (to the right).

4 Discussion

Activation of floral organ abscission is dependent on an active IDA peptide. The IDA peptide activates a signaling pathway to abscission by binding to the transmembrane receptors pair HAE HSL2 which transduce the IDA signal to further activating cytoplasmic MAPK cascade eventually leading to cell wall degradation and cell separation. Several factors are found to act in floral organ abscission either as a part of the IDA signaling pathway or interconnected to the IDA signaling pathway. Some of the factors recently included in the IDA signaling pathway are three *KNOX* genes previously shown to be important for meristem maintenance and organ patterning. Members of the LBD family have been demonstrated to be expressed in various tissues and are believed to have the ability to form complexes with each other through the LOB domain and form protein-protein interaction to other transcription factors as well as cofactors. During meristem patterning and organ development members of the LBD TF family like AS2 and JLO have been demonstrated to negatively regulate *KNOX* genes. Other LBDs have been implicated in regulation of metabolisms and root development demonstrating the diverse roles of LBDs during plant development and plant growth. The LBD family of transcription factors consists of many more factors yet to be fully characterized. Using genetic and expression analysis *LBD37*, *LBD38*, *LBD39* and *LBD41* were investigated for their hypothesized role in floral organ abscission and their possible connection to the IDA signaling pathway.

The result of the increased expression level of *LBD37* and *LBD39* in *ida* and *haehsl2* lead to further investigation of these *LBD* genes together with two closely related LBDs, LBD38 and LBD41. The results presented here demonstrate the broad expression pattern of *LBD37*, *LBD38*, *LBD39* and *LBD41* and their broad function and involvement in various developmental processes will be addressed. Most importantly, the results presented suggest a possible role for LBDs in floral organ abscission and their role as transcription factors acting in the IDA signaling pathway will be discussed and conclusions will be drawn where possible. Finally, a summary of the results and future research to further elucidate the role of LBDs in floral organ abscission will be presented.

4.1 LBDs are likely involved in various developmental processes

Expression analyses of *promoter:GUS* presented here suggests a broad functional activity of LBD37, LBD38, LBD39 and LBD41. *LBD37-39* and *LBD41* expression have been detected by RT-PCR in tissues roots, stems, cauline leaves, shoot apex, rosette leaves, floral buds, open flowers and inflorescence organs with inflorescence stems (Matsumura et al., 2009; Shi et al., 2011). Consistent with the RT-PCR results (Matsumura et al., 2009; Shi et al., 2011) GUS and YFP reporter lines driven by the respective *LBD* promoter regions revealed activity of all the four LBDs investigated in root, AZ of floral organs, SAM and rosette leaves. In the roots of 12-day-old seedlings there was a strong expression of *LBD37*, *LBD38*, *LBD39* and *LBD41* in the vascular tissue comprising the xylem and phloem cell layers of the root and leaves and the LBDs had a similar expression pattern as JLO and they shared a similar expression in the vascular system of 12-day-old leaves as well as in the hydratodes. LBD30 and LBD18 have been found to be involved in regulation of immature tracheary elements (TE) cells that constitute xylem vessels in leaves and roots (Soyano et al., 2008), thus the results of *LBD* expression in the same tissues may indicate involvement of other LBDs in regulation of maturation of TEs as well. The expression of *LBD37*, *LBD38*, *LBD39* and *LBD41* in the elongation zone of roots may suggest involvement in enlargement of cells that lead to extension of the growing root. *LBD41* was in addition expressed in the entire meristematic zone suggesting that LBD41 may also be involved in regulation of cell division. The high expression at the base of lateral roots is consistent with the role LBD37, LBD38 and LBD39 as negative regulators of nitrogen response genes in roots like *NRTs* (Nitrate transporters), which is important in regulation of lateral root development (Rubin et al., 2009).

Even though there is a high expression in the vascular tissue (stele) of roots it is difficult to separate the different cell layers that constitute the stele. Thus staining of the different layers would be helpful in determining the expression level of the different layers. By staining the root with fuchsin the lignification of xylem can be visualized while phloem can be stained by aniline blue.

The expression pattern of the different *LBDs* in SAM was similar to that of *KNAT1* and *KNAT2* as they were present in the entire meristem, while *KNAT6* is expressed closer to the boundaries between the meristem and the forming organs.

The expression in the vascular tissue in roots, expression in the endosperm layer of mature, germinated seeds, SAM, cotyledon and leaves of 12-day-old seedlings suggests involvement of LBDs in many developmental processes in plants, especially early developmental processes.

Both GUS and YFP lines were made for detection of expression of *LBDs* mainly in the floral AZ. The YFP lines turned out to be quite weak and difficult to visualize. To improve visualization and localization of the YFP expression the floral AZ could have been dissected into different layers before investigation by microscopy. However, this is very time consuming, thus the GUS lines were the main focus in the expression analysis of LBD activity.

In the AZ of floral organs all the *LBDs* investigated peaked in expression at either position 8 (*LBD37* and *LBD39*) or 10 (*LBD38* and *LBD41*), which stayed strong until position 16. Position 8-10 represents a time for organ detachment thus the presence of LBDs at this stage indicates a role during abscission as well as a role after loss of floral organs as the expression stays strong until position 16.

Recently KNOX1 proteins previously demonstrated to be involved in regulation of cell growth and cell differentiation were found to be involved in regulation of floral organ abscission (Shi et al., 2011). The *LBDs* investigated in this thesis share overlapping expression with *KNAT1* (Shi et al., 2011) which display a higher expression level at position 8 and 10. The expression level of *KNAT2* peaks at position 10 (Shi et al., 2011) at the same position where *LBD38* and *LBD41* displays elevated expression levels, while the peak in expression level of *KNAT6* at position 6-8 (Shi et al., 2011) is more consistent with the expression pattern of *LBD37* and *LBD39* which display an elevated expression at position 8. This suggests that the LBD and KNAT1, KNAT2 and KNAT6 are active in the same positions, strengthening the possibility of regulatory interactions between the LBDs and the *KNOX* genes in floral organ abscission. Interestingly, *LBD39* displayed the highest expression level at position 6, which only lightly increased in position 8 and 10, thus strengthening the role of LBD39 in floral organ abscission.

4.2 LBD38, LBD39, LBD41 in floral organ abscission

Analyses by pBS measurements of *lbd* single and double mutant lines revealed early floral organ abscission in the double mutants *lbd38 lbd39* and *lbd41 lbd39* as well as in the single mutant lines *lbd39* and *lbd38,* though not as early as in the double mutants. Loss of one LBD rarely leads to phenotypical changes suggesting their impact is masked by redundancy. Consistent with this is the highly increased effect double mutants displayed on floral organ abscission compared to the effect of the single mutants. This suggests that LBD38, LBD39 and LBD41 can act together when suppressing floral organ abscission.

The early floral organ abscission displayed in the single mutant line, *lbd39,* and the double mutants *lbd38 lbd39*, *lbd41 lbd39* and *lbd41 lbd38* may indicae early cell wall loosening. The double mutants like the *bp* mutant displayed abscission of petals one position earlier compared to wt and had a significant reduction in petal breakstrength at position 2, 4 and 6. This presents a possibility of the LBDs acting redundantly to repressors abscission at the same stage as KNAT1. The double mutant lines that displayed the highest significant reduction in abscission were the double mutants *lbd38 lbd39* and *lbd41 lbd39* sharing the loss of *LBD39*. Loss of *LBD39* displayed a significant reduction in pBS at position 6 indicating that *lbd39* alone cause early abscission, although *lbd39* in combination with loss of *LBD41* or *LBD38,* give a stronger reduction in pBS at position 6. These results, in addition to *proLBD39:GUS* displaying the strongest expression at position 6 in the expression analysis of floral AZs, indicates a central role of LBD39 in regulation of floral organ abscission. Furthermore, as loss of more than one *LBD* increases the impact on floral organ abscission the likeliness of LBDs acting redundantly further increases.

Abscission occurs after anthesis, thus AZ likely becomes competent to respond to abscission signals shortly after pollination. Before abscission of flowers there is a rounding of AZ cells. Factors acting as inhibitors of abscission like the KNOX1 protein KNAT1 and LRR-LRKs EVR, CST and SERK1 all cause increased enlargement of AZ cells when mutated either alone or in combination with loss of *NEV*. Thus, these factors also likely act as suppressors of cell enlargement (Leslie et al., 2010; Lewis et al., 2010; Burr et al., 2011; Shi et al., 2011). As *lbd* double mutants *lbd38 lbd39* and *lbd41 lbd39,* like *KNAT1* mutant, revealed abscission approximately two positions earlier than in wt and since expansion of separating cells apparently correlates with the timing of abscission it would be interesting to investigate a

potential enlargement of the AZ cells of the *lbd* double mutants (Leslie et al., 2010; Shi et al., 2011).

To investigate AZ cell size and structure at different positions along the inflorescence Scanning Electron Microscopy (SEM) could be utilized. SEM uses electrons instead of light by scanning the sample with a beam of electrons excite the atoms of the sample emitting more or less secondary electrons depending on the surface that is detected and transformed into micographs, structural images. SEM provides a much higher resolution (<1 nm) than other microscopes using light, it produce largely magnified images with high clarity and allow focus on a larger area of the sample. The images produced contain information about the structure of the surface as well as the composition. Due to the structural complexity of the floral AZ all the advantages of SEM listed are very useful when investigating AZ architecture.

4.3 LBD38, LBD39 and LBD41 in *KNOX* regulation

The LBD family members AS2 and JLO act as repressors of *KNOX1* genes during the development of leaf primordia and meristem-to-organ boundaries patterning and are expressed in the primordia and the boundary between the organ and the meristem, respectively (Xu et al., 2003; Borghi et al., 2007; Iwakawa et al., 2007; Guo et al., 2008; Rast and Simon, 2012). Floral AZs are implied to derive from meristem-to organ boundaries of floral meristems after the formation of floral organs, thus increasing the possibility of LBDs acting as regulators of *KNOX* genes involved in floral organ abscission as well. In line with this, qRT-PCR results provided here demonstrate an increased level of *KNAT1* and *KNAT6* expression in the *lbd* single mutants. *KNAT6*, which is mainly found in the meristem-to- organ boundary, displayed the highest elevation of expression. The expression level was measured in the total amount of RNA derived from position 4, 6 and 8 along the inflorescence, thus indicating repression of *KNOX* genes by LBDs in the inflorescence organs at a time where abscission is initiated. As the timing of abscission was more strongly affected in the double mutant lines, than in the *lbd* single mutant lines, an investigation of *KNOX* expression level in the *lbd* double mutants and even triple mutants would be of great interest.

Consistent with the qRT-PCR results demonstrating elevated *KNAT1* in *lbd39* mutant, GUS assessed *KNAT1* expression was elevated in the *lbd38 lbd39* double mutant. This suggests negative regulation of *KNAT1* by LBDs. However, this is not in line with the hypothesis presented as the LBDs were hypothesized only to be involved in *KNAT2* and *KNAT6* repression, acting parallel to KNAT1 when negatively regulating *KNAT2* and *KNAT6*. However, the hypothesis was supported by the pBS results where *lbd38 lbd39* and especially *lbd41 lbd39* showed early abscission like the *bp-3(knat1)* mutant. Previously characterized LBDs have been shown to regulate *KNAT1*, *KNAT2* and *KNAT6* so it is possible that LBD39 together with either LBD41 or LBD38 also are involved in repression of the *KNAT1*.

In *jlo* mutant *proKNAT1:GUS* expression had expanded into the basis of organ primordia which suggested that JLO acted in restriction of *KNAT1* expression (Rast and Simon, 2012). In the floral AZ of *lbd38 lbd39* there was an increase in *KNAT1:GUS* expression compared to wt and expanded beyond the base of emerging lateral root as well as down the receptacle and pedicel from the AZ. Thus, it could be that LBD38 and LBD39 are involved in restriction of KNAT1 expression in the AZ and at the base of lateral roots.

In line with the hypothesis and the elevated *KNAT6* expression *KNAT6:GUS* expression in *lbd38 lbd39* showed elevated expression at position 2 and 4 along the inflorescence. This also fits with the early abscission detected in the *lbd38 lbd39* double mutant; however the breakstrength did not show a significantly reduction at position 2. Even so, the elevated expression might not be sufficient to affect abscission as early as position 2, but that the sustained increase in expression could have caused the early abscission seen at position 6 in *lbd38 lbd39*. Surprisingly the expression decreased at position 6 - 8 and at position 10 the expression was much lower compared to wt which suggests that LBD38 and LBD39 directly or indirectly cause a down regulation of *KNAT6* after initiation of cell wall loosening.

AS2 and JLO can together with AS1 form a tretrameric complex that negatively regulates *KNAT1*, but thetertameric complex are also able to positively regulate *PIN* genes. Furthermore, the dimeric complex AS2/AS1 are able to regulate *KNOX* genes in leaf development (Xu et al., 2003; Borghi et al., 2007; Guo et al., 2008; Rast and Simon, 2012). LBD37 and LBD41 have the ability to interact with to TOPLESS (TPL) and TPL–related (TPR) corepressors (Causier et al., 2012) and LBD37, LBD38 and LBD39 likely act together as repressors of nitrogen-starvation induced genes (Rubin et al., 2009). Thus the LBDs can act as both activators and repressors by forming various complexes with other LBDs and other

TFs, like members of the HLH family as well as cofactors. With this in mind it is not impossible that LBD38 and LBD39 acts as both activators and repressors of *KNOX* genes at different stages during abscission by forming larger complexes with other TFs or cofactors in order to maintain the appropriate level of *KNOX* during the different stages of abscission. To further elucidate this hypothesis, studies of protein-protein interaction as well as protein-DNA interaction will be of importance.

To investigate potential interaction between the LBDs investigated in this thesis and the potential interaction between the LBDs and the KNOX proteins involved in IDA signaling pathway a mating experiment like yeast two-hybrid can be utilized. Yeast two-hybrid has already been used to investigate interaction between other LBD with great success. The yeast two-hybrid is based on the indirect binding of the Gal 4 activation domain (AD) and the GAL4 binding domain (BD), which lead to transcription of a reporter gene downstream of the binding sequence (UAS) to which BD binds. A MATa strain containing a pray vector with the proteins coding sequence fused to AD is mated with MATα containing a bait vector containing another protein or a protein binding domain fused with BD. If the proteins interact the AD will be in proximity to BD leading to transcription of the reporter gene which is selected for.

As AS2 have been found to be able to bind *KNOX* promoter region when in a complex with AS1 it would be interesting to investigate the possibility of LBD37, LBD38, LBD39 or LBD41 to bind *KNOX* promoter regions either directly or indirectly through binding of another TF. Electrophoretic mobility shift assays (EMSAs) could in this case be used. In this method the ability of a single protein or a protein complex to bind to a given DNA or RNA complex are investigated by elechrophoretic separation with the same principle as gel electrophorese: if the protein is able to bind to the DNA fragment the size of the complex will be larger than the DNA fragment alone, thus the protein-DNA complex will shift to a higher position on the gel. If a protein binds better to the fragment when in complex with another protein the size will further increase and appear even higher on the gel.

4.4 LBDs and the IDA signaling pathway

LBDs are expressed in AZs similar to that of *IDA* and other genes in IDA signaling. In addition, LBDs and IDA have overlapping expression in various tissues, such as endosperm and base of lateral roots. Our qRT-PCR results showed an up regulation of *LBD37* and *LBD39* in *ida* and *haehsl2*. This raises questions of whether the same factors are involved in different cell separation processes and whether LBDs act in the IDA signaling pathway acting as regulators of *KNOX*.

In contrast to the qRT-PCR results the *proLBD37:GUS* expression was severely decreased and *proLBD38:GUS* expression was absent in the floral AZs of the *ida* mutant. Furthermore, *proLBD39:GUS* expression was absent in the floral AZs of *hae hsl2*. When staining the seedlings of the three triple mutants, the roots of *proLBD38:GUS ida* and *proLBD39:GUS ida* were stained, however, there was no significant expression in the aerial part of the seedling, in line with the absent expression in the floral AZ of full grown plants. With qRT-PCR there are often problems with the specificity of the primers used. This could explain why there was detected elevated *LBD39* expression in the *ida* and *hae hsl2* mutants, suggesting that *LBD39* could be positively regulated by IDA. The *LBD38* expression level was not investigated in the qRT-PCR and as the roots of *proLBD38:GUS ida* were quickly stained, it seems likely that IDA positively regulates *LBD38*. If the *LBDs* are positively regulated by IDA, they must be positively regulated by HAE HSL2 as well since IDA signals through HAE/HSL2 (Butenko et al., 2003; Stenvik et al., 2006; Stenvik et al., 2008; Matsubayashi, 2011; Butenko et al., 2014). The *proLBD39:GUS* expression in *hae hsl2* was absent in both the AZ and in the entire seedling. Since there is a broader overlapping expression between *LBDs* and *HAE HSL2* in roots, the lack of expression in *hae hsl2* mutant could be due to deficient activation by HAE and HSL2 or, most likely, as the expression of *LBDs* and *HAE* and *HSL2* do not fully overlap, it could be due to total silencing of the *LBD39* promoter.

Overexpression of *IDA* lead to premature abscission, but in *hae hsl2* mutants, which, like the *ida* mutant, retain their floral organ indefinitely, the overexpression of *IDA* has no impact on the *hae hsl2* mutant phenotype (Butenko et al., 2003; Stenvik et al., 2006; Stenvik et al., 2008). Loss of *KNAT1* could almost completely rescue the *hae hsl2* phenotype, however some of the stamens were still attached to a few siliques (Shi et al., 2011). Preliminary pBS results of *lbd38 lbd39* showed reduced petal breakstrength compared to *hae hsl2* at position 2-14 with a highly significant reduction at position 6-8 and the floral organs of *hae hsl2 lbd38*

lbd39 appeared to be more loosely attached to the floral AZ than the floral organs of *hae hsl2*. However, as in *hae hsl2*, the floral organs fail to abscise in *hae hsl2 lbd38 lbd39.* This again are in line with the elevated expression of *LBD39* in *ida* and *hae hsl2*, suggesting that HAE and HSL2 cause negative regulation of *LBD38* and *LBD39.* If the qRT-PCR results are correct, the lack of expression in the aerial parts of the GUS lines could be due to silencing of *LBD39* and *LBD38* expression in the aerial part of the plant. As all of the *promoter:GUS lines* were quickly stained, the expression level of LBDs at the floral AZ are likely very high and a further increase in expression caused by the absence of *IDA* may have cause silencing of the *LBD*. In this case the LBDs would likely be negatively regulated by IDA and HAE HSL2, as hypothesized. The inability of *lbd38 lbd39* to fully rescue *hae hsl2* phenotype may suggest involvement of other inhibitors of abscission, such as KNAT1 or other LBDs that prevents the floral organ from fully abscising.

As IDA signals for abscission, an inhibitor acting downstream of IDA-HAEHSL2 would be expected to be up-regulated in a *ida* and *hae hsl2* mutant like the qRT-PCR results showed. However, the LBDs could be regulated at protein level, which will not be detected by qRT-PCR or GUS.

If LBDs are positively regulated by IDA, the LBDs could still act as inhibitors of abscission. In this case the LBDs could be induced by IDA to act as breaks during abscission thus regulating the rate at which abscission occur. This coincides with the elevated expression of *KNAT6* as well as *KNAT1* in *lbd38 lbd39,* as KNAT1 act as an inhibitor while KNAT6 act in favor of abscission.

It would be necessary to further investigate the connection between IDA and HAE HSL2 and the LBDs.

4.5 Summary and future aspects

proLBD37:GUS, proLBD38:GUS, proLBD39:GUS and *proLBD41:GUS* all showed expression in the floral AZ, as well as in vasculature of the plant and SAM seedlings. The expression in the floral AZ peaked at a lower position (8-10) than anticipated, however they all showed expression at earlier positions (2-6) and showed an over lapping expression to an inhibitor of abscission, *KNAT1* (Shi et al., 2011). This in addition to the pBS results presented here suggest a role of LBD38, LBD39 and LBD41 as inhibitors of floral organ abscission.

Moreover, the effect of *lbd38 lbd39* on *KNOX* expression suggests a role in *KNOX* regulation. As the LBDs might act as repressors of *KNAT1* as well as *KNAT6*, LBDs might not be a part of the IDA signaling pathway in a way that fits entirely with the hypothesis presented. Since the two *hae hsl2 lbd38 lbd39* mutants showed a reduction in petal breakstrength at position 2-6 compared to the *hae hsl2* (Stenvik et al., 2008) and since the breakstrength at position 6 in the two quadruple mutants was reduced to a level similar to that in wt, it would be possible that there is a connection between the IDA signaling pathway and the LBDs and that HAE HSL2 cause repression of LBDs during floral organ abscission. Although, there are some contradicting results regarding whether the *LBDs* are positively or negatively regulated by IDA, HAE and HSL2.

To further elucidate the roles of LBDs in floral organ abscission it would be of interest to further investigate the function of LBD39 in floral organ abscission as *lbd39* gave the most interesting results either alone or in combination with one of the other LBDs investigated. It would be of interest to investigate a potential role of LBD37 as well, since LBD37 was quickly excluded from further studies due to the T-DNA being inserted in 3'UTR region of *lbd37*. It would be necessary to further investigate the double mutant *lbd41 lbd39* as this showed the lowest pBS values at position 6. Finally investigation of *lbd* double mutants in *KNOX* double mutant would be of importance as well as an investigation of expression of *KNAT2* in the double mutant lines even though the qRT-PCR results did not show a significant increase in expression in the single mutants.

Other experiments to further advance our understanding of the role of LBDs in floral organ abscission have been suggested: (1) investigation of the effect single and higher order *lbd* mutant have on the floral AZ architecture, (2) investigate *KNAT* expression in higher order mutants of *lbds*, (3) interaction studies to investigate dimer formation between LBDs, other TFs and cofactors, as well as the potential of the LBDs to interact with *KNOX* promoter region.

References

Aalen, R., Wildhagen, M., Stø, I., and Butenko, M. (2013). IDA: a peptide ligand regulating cell separation processes in Arabidopsis. Journal of experimental botany **64,** 5253-5261.

Arabidopsis Genome Initiative. (2000). Analysis of the genome sequence of the flowering plant *Arabidopsis thaliana*. Nature **408,** 796-815.

Barton, M.K., and Poethig, R.S. (1993). Formation of the shoot apical meristem in *Arabidopsis thaliana*: an analysis of development in the wild type and in the shoot meristemless mutant. Development **119,** 823.

Basu, M., González-Carranza, Z., Azam Ali, S., Tang, S., Shahid, A., and Roberts, J. (2013). The manipulation of auxin in the abscission zone cells of Arabidopsis flowers reveals that indoleacetic acid signaling is a prerequisite for organ shedding. Plant physiology **162,** 96-106.

Bleecker, A.B., and Patterson, S.E. (1997). Last exit: senescence, abscission, and meristem arrest in Arabidopsis. Plant Cell **9,** 1169-1179.

Borghi, L., Bureau, M., and Simon, R. (2007). Arabidopsis JAGGED LATERAL ORGANS is expressed in boundaries and coordinates KNOX and PIN activity. Plant Cell **19,** 1795-1808.

Burr, C., Leslie, M., Orlowski, S., Chen, I., Wright, C., Daniels, M., and Liljegren, S. (2011). CAST AWAY, a membrane-associated receptor-like kinase, inhibits organ abscission in Arabidopsis. Plant physiology **156,** 1837-1850.

Butenko, M., Stenvik, G.-E., Alm, V., Saether, B., Patterson, S., and Aalen, R. (2006). Ethylene-dependent and -independent pathways controlling floral abscission are revealed to converge using promoter::reporter gene constructs in the *ida* abscission mutant. Journal of experimental botany **57,** 3627-3637.

Butenko, M., Butenko, A., Vie, T., Brembu, R., Aalen, A., and Bones. (2009). Plant peptides in signalling: looking for new partners. Trends in plant science **14,** 255-263.

Butenko, M., Patterson, S., Grini, P., Stenvik, G.-E., Amundsen, S., Mandal, A., and Aalen, R. (2003). Inflorescence deficient in abscission controls floral organ abscission in Arabidopsis and identifies a novel family of putative ligands in plants. Plant Cell **15,** 2296-2307.

Butenko, M., Wildhagen, M., Albert, M., Jehle, A., Kalbacher, H., Aalen, R., and Felix, G. (2014). Tools and Strategies to Match Peptide-Ligand Receptor Pairs. Plant Cell **26,** 1838-1847.

Bürglin, T.R. (1997). Analysis of *TALE superclass homeobox* genes (*MEIS, PBC, KNOX, Iroquois, TGIF*) reveals a novel domain conserved between plants and animals. Nucleic acids research **25,** 4173-4180.

Byrne, M., Simorowski, J., and Martienssen, R. (2002). ASYMMETRIC LEAVES1 reveals *knox* gene redundancy in Arabidopsis. Development **129,** 1957-1965.

Byrne, R.A., Martienssen, M., Byrne, R., Barley, M., Curtis, J., Arroyo, M., Dunham, A., and Hudson. (2000). Asymmetric leaves1 mediates leaf patterning and stem cell function in Arabidopsis. Nature **408,** 967-971.

Cai, S., and Lashbrook, C. (2008). Stamen abscission zone transcriptome profiling reveals new candidates for abscission control: enhanced retention of floral organs in transgenic plants overexpressing Arabidopsis ZINC FINGER PROTEIN2. Plant physiology **146,** 1305-1321.

Causier, B., Ashworth, M., Guo, W., and Davies, B. (2012). The TOPLESS interactome: a framework for gene repression in Arabidopsis. Plant physiology **158,** 423-438.

Cho, S., Larue, C., Chevalier, D., Wang, H., Jinn, T.-L., Zhang, S., and Walker, J. (2008). Regulation of floral organ abscission in *Arabidopsis thaliana*. Proceedings of the National Academy of Sciences of the United States of America **105,** 15629-15634.

Clough, S., Clough, A., and Bent. (1998). Floral dip: a simplified method for*Agrobacterium*-mediated transformation of*Arabidopsis thaliana*. Plant journal **16,** 735-743.

Cosgrove, D.J. (1998). Cell wall loosening by expansins. Plant physiology **118,** 333-339.

del Campillo, E., Campillo, A., Abdel Aziz, D., Crawford, S., and Patterson. (2004). Root cap specific expression of an endo-β-1,4-glucanase (cellulase): a new marker to study root development in Arabidopsis. Plant molecular biology **56,** 309-323.

Dellaporta, S., Dellaporta, J., Wood, J., and Hicks. (1983). A plant DNA minipreparation: Version II. Plant molecular biology reporter **1,** 19-21.

Ellenberger, T., Ellenberger, C., Brandl, K., Struhl, S., and Harrison. (1992). The GCN4 basic region leucine zipper binds DNA as a dimer of uninterrupted α Helices: Crystal structure of the protein-DNA complex. Cell **71,** 1223-1237.

Gawadi, A.G.a.A., George S., Jr. (1950). Leaf Abscission and the So-Called "Abscission Layer". American Journal of Botany**,** 172-180.

González-Carranza, Z., Elliott, K., and Roberts, J. (2007). Expression of polygalacturonases and evidence to support their role during cell separation processes in *Arabidopsis thaliana*. Journal of experimental botany **58,** 3719-3730.

González Carranza, Z., González Carranza, E., Lozoya Gloria, J., and Roberts. (1998). Recent developments in abscission: shedding light on the shedding process. Trends in plant science **3,** 10-14.

Guo, M., Thomas, J., Collins, G., and Timmermans, M.C.P. (2008). Direct repression of *KNOX* loci by the ASYMMETRIC LEAVES1 complex of Arabidopsis. Plant Cell **20,** 48-58.

Ha, C., Jun, J., and Fletcher, J. (2010). Control of Arabidopsis leaf morphogenesis through regulation of the YABBY and KNOX families of transcription factors. Genetics **186,** 197-206.

Ha, C., Jun, J., Nam, H., and Fletcher, J. (2007). BLADE-ON-PETIOLE 1 and 2 control Arabidopsis lateral organ fate through regulation of LOB domain and adaxial-abaxial polarity genes. Plant Cell **19,** 1809-1825.

Ha, C., Kim, G.-T., Kim, B., Jun, J., Soh, M., Ueno, Y., Machida, Y., Tsukaya, H., and Nam, H. (2003). The *BLADE-ON-PETIOLE 1* gene controls leaf pattern formation through the modulation of meristematic activity in Arabidopsis. Development **130,** 161-172.

Hepworth, S., Zhang, Y., McKim, S., Li, X., and Haughn, G. (2005). BLADE-ON-PETIOLE-dependent signaling controls leaf and floral patterning in Arabidopsis. Plant Cell **17,** 1434-1448.

Husbands, A., Bell, E., Shuai, B., Smith, H.M.S., and Springer, P. (2007). LATERAL ORGAN BOUNDARIES defines a new family of DNA-binding transcription factors and can interact with specific bHLH proteins. Nucleic acids research **35,** 6663-6671.

Ikezaki, M., Kojima, H., Sakakibara, S., Kojima, Y., Ueno, C., Machida, Y., and Machida. (2010). Genetic networks regulated byASYMMETRIC LEAVES1(AS1) andAS2in leaf development in*Arabidopsis thaliana*:*KNOX*genes control five morphological events. Plant journal **61,** 70-82.

Iwakawa, H., Iwakawa, M., Iwasaki, S., Kojima, Y., Ueno, T., Soma, H., Tanaka, E., Semiarti, Y., Machida, C., and Machida. (2007). Expression of the*ASYMMETRIC LEAVES2*gene in the adaxial domain of Arabidopsis leaves represses cell proliferation in this domain and is critical for the development of properly expanded leaves. Plant journal **51,** 173-184.

Iwakawa, H., Ueno, Y., Semiarti, E., Onouchi, H., Kojima, S., Tsukaya, H., Hasebe, M., Soma, T., Ikezaki, M., Machida, C., and Machida, Y. (2002). The *ASYMMETRIC LEAVES2* gene of *Arabidopsis thaliana*, required for formation of a symmetric flat leaf lamina, encodes a member of a novel family of proteins characterized by cysteine repeats and a leucine zipper. Plant & Cell Physiology **43,** 467-478.

Jarvis, M.C., Briggs, S.P.H., and Knox, J.P. (2003). Intercellular adhesion and cell separation in plants. Plant, cell and environment **26,** 977-989.

Jinn, T.L., Stone, J.M., and Walker, J.C. (2000). HAESA, an Arabidopsis leucine-rich repeat receptor kinase, controls floral organ abscission. Genes & development **14,** 108-117.

Jun, J., Ha, C., and Fletcher, J. (2010). BLADE-ON-PETIOLE1 coordinates organ determinacy and axial polarity in arabidopsis by directly activating *ASYMMETRIC LEAVES2*. Plant Cell **22,** 62-76.

Kawade, K., Kawade, G., Horiguchi, T., Usami, M., Hirai, H., and Tsukaya. (2013). ANGUSTIFOLIA3 Signaling Coordinates Proliferation between Clonally Distinct Cells in Leaves. Current biology **23,** 788-792.

Khan, M., Xu, M., Murmu, J., Tabb, P., Liu, Y., Storey, K., McKim, S., Douglas, C., and Hepworth, S. (2012). Antagonistic interaction of BLADE-ON-PETIOLE1 and 2 with BREVIPEDICELLUS and PENNYWISE regulates Arabidopsis inflorescence architecture. Plant physiology **158,** 946-960.

Kim, D.-H., Woo, J.-M., Kim, S.-Y., Lee, W., Chung, Y.-H., and Moon. (2011). Arabidopsis MKK4 mediates osmotic-stress response via its regulation of MPK3 activity. Biochemical and biophysical research communications **412,** 150-154.

Kumpf, R., Shi, C.-L., Larrieu, A., StÃƒ, I., Butenko, M., PÃret, B., Riiser, E., Bennett, M., and Aalen, R. (2013). Floral organ abscission peptide IDA and its HAE/HSL2 receptors control cell separation during lateral root emergence. Proceedings of the National Academy of Sciences of the United States of America **110,** 5235-5240.

Lease, K., Cho, S.K., and Walker, J. (2006). A petal breakstrength meter for *Arabidopsis* abscission studies. Plant Methods.

Leslie, M., Lewis, M., Youn, J.-Y., Daniels, M., and Liljegren, S. (2010). The EVERSHED receptor-like kinase modulates floral organ shedding in Arabidopsis. Development **137,** 467-476.

Lewis, M., Leslie, E., Fulcher, L., Darnielle, P., Healy, J.-Y., Youn, S., and Liljegren. (2010). The SERK1 receptor-like kinase regulates organ separation in Arabidopsis flowers. Plant journal **62,** 817-828.

Liljegren, S., and Liljegren. (2012). Organ abscission: exit strategies require signals and moving traffic. Current opinion in plant biology **15,** 670-676.

Liljegren, S., Leslie, M., Darnielle, L., Lewis, M., Taylor, S., Luo, R., Geldner, N., Chory, J., Randazzo, P., Yanofsky, M., and Ecker, J. (2009). Regulation of membrane trafficking and organ separation by the NEVERSHED ARF-GAP protein. Development **136,** 1909-1918.

Lin, W.-c., Shuai, B., and Springer, P. (2003). The Arabidopsis LATERAL ORGAN BOUNDARIES-domain gene *ASYMMETRIC LEAVES2* functions in the repression of *KNOX* gene expression and in adaxial-abaxial patterning. Plant Cell **15,** 2241-2252.

Liu, B., Butenko, M., Shi, C.-L., Bolivar, J., Winge, P., Stenvik, G.-E., Vie, A., Leslie, M., Brembu, T., Kristiansen, W., Bones, A., Patterson, S., Liljegren, S., and Aalen, R. (2013). NEVERSHED and INFLORESCENCE DEFICIENT IN ABSCISSION are differentially required for cell expansion and cell separation during floral organ abscission in *Arabidopsis thaliana*. Journal of experimental botany **64,** 5345-5357.

Lodha, M., Marco, C., and Timmermans, M.C.P. (2013). The ASYMMETRIC LEAVES complex maintains repression of *KNOX homeobox* genes via direct recruitment of Polycomb-repressive complex2. Genes & development **27,** 596-601.

Long, J., Long, E., Moan, J., Medford, M.K., and Barton. (1996). A member of the KNOTTED class of homeodomain proteins encoded by the *STM* gene of Arabidopsis. Nature **379,** 66-69.

Mangeon, A., Mangeon, W.-c., Lin, P., and Springer. (2012). Functional divergence in the *Arabidopsis LOB-domain* gene family. Plant signaling & behavior **7,** 1544-1547.

Martin, C.E., Martin, a.D.J., and von, W. (2000). Leaf Epidermal Hydathodes and the Ecophysiological Consequences of Foliar Water Uptake in Species of Crassula from the Namib Desert in Southern Africa. Plant biology **2,** 229-242.

Matsubayashi, Y. (2011). Small Post-Translationally Modified Peptide Signals in Arabidopsis. The Arabidopsis Book.

Matsumura, Y., Matsumura, H., Iwakawa, Y., Machida, C., and Machida. (2009). Characterization of genes in theASYMMETRIC LEAVES2/LATERAL ORGAN BOUNDARIES(AS2/LOB) family in*Arabidopsis thaliana*, and functional and molecular comparisons betweenAS2and other family members. Plant journal **58,** 525-537.

McKim, S., Stenvik, G.-E., Butenko, M., Kristiansen, W., Cho, S., Hepworth, S., Aalen, R., and Haughn, G. (2008). The *BLADE-ON-PETIOLE* genes are essential for abscission zone formation in Arabidopsis. Development **135,** 1537-1546.

Meinke, D.W., Cherry, J.M., Dean, C., Rounsley, S.D., and Koornneef, M. (1998). *Arabidopsis thaliana*: a model plant for genome analysis. Science **282,** 662-662, 682.

Mele, G., Ori, N., Sato, Y., and Hake, S. (2003). The knotted1-like homeobox gene *BREVIPEDICELLUS* regulates cell differentiation by modulating metabolic pathways. Genes & development **17,** 2088-2093.

Meng, L.-S., Meng, X.-D., Sun, F., Li, H.-L., Liu, Z.-H., Feng, J., and Zhu. (2010). Modification of flowers and leaves in Cockscomb (Celosia cristata) ectopically expressing Arabidopsis *ASYMMERTIC LEAVES2-LIKE38 (ASL38/LBD41)* gene. Acta physiologiae plantarum **32,** 315-324.

Müller, J., Müller, Y., Wang, R., Franzen, L., Santi, F., Salamini, W., and Rohde. (2001). In vitro interactions between barley TALE homeodomain proteins suggest a role for protein-protein associations in the regulation of *KNOX* gene function. Plant journal **27,** 13-23.

Norberg, M., Holmlund, M., and Nilsson, O. (2005). The BLADE ON PETIOLE genes act redundantly to control the growth and development of lateral organs. Development **132,** 2203-2213.

Ogawa, M., Kay, P., Wilson, S., and Swain, S. (2009). ARABIDOPSIS DEHISCENCE ZONE POLYGALACTURONASE1 (ADPG1), ADPG2, and QUARTET2 are Polygalacturonases required for cell separation during reproductive development in Arabidopsis. Plant Cell **21,** 216-233.

Okushima, Y., Fukaki, H., Onoda, M., Theologis, A., and Tasaka, M. (2007). ARF7 and ARF19 regulate lateral root formation via direct activation of *LBD/ASL* genes in Arabidopsis. Plant Cell **19,** 118-130.

Ori, N., Eshed, Y., Chuck, G., Bowman, J.L., and Hake, S. (2000). Mechanisms that control *KNOX* gene expression in the Arabidopsis shoot. Development **127,** 5523-5532.

Osborne, D., Osborne, P., and Morgan. (1989). Abscission. Critical reviews in plant sciences **8,** 103-129.

Patterson, S.E. (2001). Cutting loose. Abscission and dehiscence in Arabidopsis. Plant physiology **126,** 494-500.

Pfaffl, M.W. (2001). A new mathematical model for relative quantification in real-time RT-PCR. Nucleic acids research **29,** e45-e45.

Phelps Durr, T., Thomas, J., Vahab, P., and Timmermans, M.C.P. (2005). Maize rough sheath2 and its Arabidopsis orthologue ASYMMETRIC LEAVES1 interact with HIRA, a predicted histone chaperone, to maintain *KNOX* gene silencing and determinacy during organogenesis. Plant Cell **17,** 2886-2898.

Pickersgill, B. (2007). Domestication of plants in the Americas: insights from Mendelian and molecular genetics. Annals of botany **100,** 925-940.

Ragni, L., Belles Boix, E., Günl, M., and Pautot, V. (2008). Interaction of KNAT6 and KNAT2 with BREVIPEDICELLUS and PENNYWISE in Arabidopsis inflorescences. Plant Cell **20,** 888-900.

Rast, M., and Simon, R. (2012). Arabidopsis JAGGED LATERAL ORGANS acts with ASYMMETRIC LEAVES2 to coordinate *KNOX* and *PIN* expression in shoot and root meristems. Plant Cell **24,** 2917-2933.

Roberts, J., and Roberts. (2000). Cell Separation Processes in Plants—Models, Mechanisms and Manipulation. Annals of botany **86,** 223-235.

Roberts, J., Roberts, K., Elliott, Z., and Gonzalez, C. (2002). ABSCISSION, DEHISCENCE, ANDOTHERCELLSEPARATIONPROCESSES. Annual review of plant biology **53,** 131-158.

Rubin, G., Tohge, T., Matsuda, F., Saito, K., and Scheible, W.-R. (2009). Members of the LBD family of transcription factors repress anthocyanin synthesis and affect additional nitrogen responses in Arabidopsis. Plant Cell **21,** 3567-3584.

Sarojam, R., Sappl, P., Goldshmidt, A., Efroni, I., Floyd, S., Eshed, Y., and Bowman, J. (2010). Differentiating Arabidopsis shoots from leaves by combined YABBY activities. Plant Cell **22,** 2113-2130.

Semiarti, E., Ueno, Y., Tsukaya, H., Iwakawa, H., Machida, C., and Machida, Y. (2001). The *ASYMMETRIC LEAVES2* gene of *Arabidopsis thaliana* regulates formation of a symmetric lamina, establishment of venation and repression of meristem-related homeobox genes in leaves. Development **128,** 1771-1783.

Sexton, R., Sexton, J.A., and Roberts. (1982). Cell Biology of Abscission. Annual review of plant physiology **33,** 133-162.

Shi, C.-L., Stenvik, G.-E., Vie, A., Bones, A., Pautot, V.r., Proveniers, M., Aalen, R., and Butenko, M. (2011). Arabidopsis class I KNOTTED-like homeobox proteins act downstream in the IDA-HAE/HSL2 floral abscission signaling pathway. Plant Cell **23,** 2553-2567.

Shuai, B., Reynaga-Peña, C., and Springer, P. (2002). The *Lateral Organ Boundaries* gene defines a novel, plant-specific gene family. Plant physiology **129,** 747-761.

Siegfried, K.R., Eshed, Y., Baum, S.F., Otsuga, D., Drews, G.N., and Bowman, J.L. (1999). Members of the *YABBY* gene family specify abaxial cell fate in Arabidopsis. Development **126,** 4117-4128.

Soyano, T., Thitamadee, S., Machida, Y., and Chua, N.-H. (2008). ASYMMETRIC LEAVES2-LIKE19/LATERAL ORGAN BOUNDARIES DOMAIN30 and ASL20/LBD18 regulate tracheary element differentiation in Arabidopsis. Plant Cell **20,** 3359-3373.

Stahl, Y., Stahl, R., and Simon. (2010). Plant primary meristems: shared functions and regulatory mechanisms. Current opinion in plant biology **13,** 53-58.

Stefano, G., Stefano, L., Renna, M., Rossi, E., Azzarello, S., Pollastri, F., Brandizzi, F., Baluska, S., and Mancuso. (2010). AGD5 is a GTPase-activating protein at the trans-Golgi network. Plant journal **64,** 790-799.

Stenvik, G.-E., Butenko, M., Urbanowicz, B., Rose, J.K.C., and Aalen, R. (2006). Overexpression of *INFLORESCENCE DEFICIENT IN ABSCISSION* activates cell separation in vestigial abscission zones in Arabidopsis. Plant Cell **18,** 1467-1476.

Stenvik, G.-E., Tandstad, N., Guo, Y., Shi, C.-L., Kristiansen, W., Holmgren, A.r., Clark, S., Aalen, R., and Butenko, M. (2008). The EPIP peptide of INFLORESCENCE DEFICIENT IN ABSCISSION is sufficient to induce abscission in arabidopsis through the receptor-like kinases HAESA and HAESA-LIKE2. Plant Cell **20,** 1805-1817.

Swarup, K., Swarup, E., Benková, R., Swarup, I., Casimiro, B., Péret, Y., Yang, G., Parry, E., Nielsen, I., De Smet, S., Vanneste, M., Levesque, D., Carrier, N., James, V., Calvo, K., Ljung, E., Kramer, R., Roberts, N., Graham, S., Marillonnet, K., Patel, J.D.G., Jones, C., Taylor, D., Schachtman, S., May, G., Sandberg, P., Benfey, J., Friml, I., Kerr, T., Beeckman, L., Laplaze, M., and Bennett. (2008). The auxin influx carrier LAX3 promotes lateral root emergence. Nature Cell Biology **10,** 946-954.

Taylor, J., Taylor, C., and Whitelaw. (2001). Signals in abscission. New phytologist **151,** 323-340.

Tena, G., Tena, T., Asai, W.-L., Chiu, J., and Sheen. (2001). Plant mitogen-activated protein kinase signaling cascades. Current opinion in plant biology **4,** 392-400.

van Nocker, S., and van, N. (2009). Development of the abscission zone. Stewart Postharvest Review **5,** 1-6.

Wang, X.-Q., Wang, W.-H., Xu, L.-G., Ma, Z.-M., Fu, X.-W., Deng, J.-Y., Li, Y.-H., and Wang. (2006). Requirement of KNAT1/BP for the Development of Abscission Zones in *Arabidopsis thaliana*. Journal of integrative plant biology **48,** 15-26.

Xu, L., Dong, A., Sun, Y., Pi, L., Xu, Y., and Huang, H. (2003). Novel as1 and as2 defects in leaf adaxial-abaxial polarity reveal the requirement for ASYMMETRIC LEAVES1 and 2 and ERECTA functions in specifying leaf adaxial identity. Development **130,** 4097-4107.

Žádníková, P., and Simon, R. (2014). How boundaries control plant development. Current opinion in plant biology **17,** 116-117.

Appendix

Appendix 1: List of abbreviations

°C	degrees celcius
2-ME	mercaptoethanol
aa	amino acid
AD	activation domain
Agrobacterium	*Agrobacterium tumefaciens*
Arabidopsis	*Arabidopsis thaliana*
AS	ASYMMETRIC LEAVES
AZ	Abscission zone
BD	binding domain
bHLH	basic Helix-Loop-Helix
BOP	BLADE-ON-PETIOLE
bp	base pair
BP	BREVIPEDICELLUS
ccdB	toxin encoded by the ccd operon
cDNA	complementary DNA
CO	Cortical
Col	Colombia
CST	CAST AWAY
CWR	cell wall remodelling
ddH_2O	double-destilled water
dH_2O	destilled water
DMF	dimethylformamide
dNTP	deoxynucleotide triphosphate
DOV	Depth of view
E. coli	*Escherichia coli*
EB	Elution buffer
EDTA	Ethylenediaminetetraacetic acid
EMSA	Electrophoretic mobility shift assays
EN	Endodermal
EP	Epidermal
EPIP	Extended PIP
EtBr	Ethidium bromide
EtOH	Ethanol
EVR	EVERSHED
EXP	expansine
FOV	Field of view
FRET	Fluorescence Resonance Energy Transfer
Gent	Gentamycin
GUS	β-glucoronidase
h	hour
HAE	HAESA
HSL2	HAESA-LIKE 2
HYG	Hygromycin
IAA	indole-3-acetic acid

IDA	INFLORESCENCE DEFICIENT IN ABSCISSION
IDL	IDA-LIKE
JLO	JAGGED LATERAL ORGAN
KAc	potassium acetate
Km	Kanamycin
KNAT	KNOTTED-LIKE FROM ARABIDOPSIS THALIANA
KNOX	KNOTTED-like homeobox
LB	10 g/l Peptone, 5 g/l Yeast extract, 10 g/l NaCl
LB	Left border
LBD	LATERAL ORGAN BOUNDARY DOMAIN
LOB	LATERAL ORGAN BOUNDARIES domain
LR	Lateral root
LRE	Lateral root emergence
LRR-RLK	Leucine-rich repeat receptor-like kinases
M	Molar
MAPK/MPK	mitogen-activated protein kinase
mg	milligram
min	minutes
MKK	MAP Kinase kinase
ml	milliliter
mRNA	messenger RNA
MS	Murashige and Skoog medium
MS-2	MS medium with 2 % sucrose
N_2	Liquid nitrogen
NaAc	Natrium acetate
NEV	NEVERSHED
ng	nanogram
O.N	over night
OD	Optical density
pBS	petal break strength
PCR	Polymerase chain reaction
PG	Polygalacturonase
PIN	Pin-formed
PNY	PENNYWISE
PRC	Polycomb-repressive complex
RB	Right border
Rif	Rifampicin
RLK	Receptor-like kinase
rpm	Revolutions per minute
RT	Reverse transcriptase
RT	room temperature
RT-PCR	Reverse transcriptase PCR
RT-qPCR	real time quantitative PCR
SAM	Shoot apical meristem
sec	seconds
SEM	Scanning Electron Microscopy
SERK1	Somatic embryogenesis receptor-like kinase1
SOC	0.5 % (w/v) yeast extract, 2 % (w/v) tryptone, 10 mM NaCl, 2.5 mM KCl, 20 mM $MgSO_4$, 20 mM glucose
Sp	Spectinomycin

ssDNA	single stranded DNA
STM	SHOOT MERISTEMLESS
TAIR	The Arabidopsis Information Resource
TF	Transcription factor
TPL	TOPPLESS
TPR	TOPPLESS-related
UAS	binding sequence of BD
UTR	untranslated region
WB	Wash buffer
wt	wild type
X-Gluc	5-bromo-4-chloro-3-indolyl ß-D-glucuronide
XTH	Xyloglucan endotransglucosylase/hydrolase
YAB	YABBY
YEB	5 g/l Beef extract, 1 g/l Yeast extract, 1 g/l Bacto Peptone, 5 g/l sucrose, pH set to 7,4 and after autoclavation addition of 2 ml 1 M MgSO4
YFP	Yellow fluorescent protein
Zeo	zeocin
λ	bacteriofag lambda
µl	mikroliter

Appendix 2: primer list

Supplemental table 1: Primers

Primer name	Sequence
RT-PCR	
qLBD37Fn	TGTGACAAGGGTGATGTGTACG
qLBD37Rn	AAACGACGTAGTTGTTAATTCGC
qLBD38Fn	CGTCTTCGTCGCTAAGTTCTTC
lbd38-2 RP	AAGCTTCGTCGGAAGTAGGAG
qLBD39F-54	TCGTCGCTAAATTCTTTGGTC
attB2ASPLBD39 stop codon	GGGGACCACTTTGTACAAGAAAGCTGGGTACCCCAAAATTTTATCATATTT
qLBD41Fn	GGAATCCGAGAGCAATGTCTC
qLBD41Rn	CCTTCTCTTCTTAACAGGTACCACA
qRT-PCR	
qKNAT1 F	TCCCATTCACATCCTCAACA
qKNAT1 R	CCCCTCCGCTGTTATTCTCT
qKNAT2-153F	CAGCGTCTGCTACAGCTCTTT
qKNAT2-153R	TCATCCGCTGCTATGTCATC
qKNAT6F	GTCTGCCAGGGGAGTTTCT
qKNAT6R	GCTACCTCATGATCACCTCCA
qLBD37F-54	CGTCTTCGTCGCTAAATTCTTC
qLBD37R-54	GCAACGACTGAAACAAAGCA
qLBD39F-54	TCGTCGCTAAATTCTTTGGTC
qLBD39R-54	CAAACAACAACGACTGAAACAAA
act2int2 antisense	CCGCAAGATCAAGACGAAGGATGC
act2int2 sense	CCCTGAGGAGCACCCAGTTCTACTC
Genotyping	
LBb1	GCGTGGACCGCTTGCTGCAACT
SALK_057939 LP	GGGCTCTCTCTCTGTGTCATG
SALK_057939 RP	GAAGCATCTGAGATCTGCACC
attB2 ASPLBD37 stop codon	GGGGACCACTTTGTACAAGAAAGCTGGGTATTGGATGCGTAACTATTTTG
qLBD38Fn	CGTCTTCGTCGCTAAGTTCTTC
lbd38-2 RP	AAGCTTCGTCGGAAGTAGGAG
SALK_011706 LP	CCCTCGGAAGCTAATTTATCG
SALK_011706 RP	CTTCTTGAATCTCCGTCGTTG
qLBD39Fn	ATGGGATGAGAGGAGATAATAAACA
lbd41 LP	CTTCATCTTCTCTCACCGTCG
lbd41 RP	GGAGAACCGGTCAAAGAGATC
LPHAE	CACCTTCCTTCTCTCCATTCC
RPHAE	GTTCGAGAAGTGACAAGCGAG
LPHSL2	CGTCTTGAGCTAGCCAACAAC

RPHSL2	GTCCAATCAAGTGGAGAAACG
ida-2 LP	TTTTGGCCACTTGAGAAATTG
ida-2 RP	GAAAATAAAAGTCGAAGGCGG
k2 LP (KNAT2)	CTCTAGCGCAAAAGTTTTTGC
k2 RP (KNAT2)	AAAGGTGATCTCGCTGCTTTC
k6 LP (KNAT6)	AGCTATTTTTCCCTTGATGGG
k6 RP (KNAT6)	TTATGGCCACAATGTTTTTGC
GUS antisense	TACATTGACGCAGGTGATCGGACGC
GUS sense	AACTGTGGAATTGATCAGCGTTGGTGG
YFP and GUS constructs/ Sequencing	
attB1 SP/LBD37/1-2535	GGGGACAAGTTTGTACAAAAAAGCAGGCTTAATCATAAATTAATCAAATGGCC
attB2 ASP/LBD37/1-2535	GGGGACCACTTTGTACAAGAAAGCTGGGTACTTTTCAGATTCAAGTTT
attB1 SP/LBD38/1-2564	GGGGACAAGTTTGTACAAAAAAGCAGGCTTAAAAGACAAAAGCAAAAAT
attB2 ASP/LBD38/1-2564	GGGGACCACTTTGTACAAGAAAGCTGGGTATATTTTCAGAAATCTTTT
attB1 SP/promoter LBD39/124-1991	GGGGACAAGTTTGTACAAAAAAGCAGGCTTAATATCAACCAAATACTGA
attB2 ASP/promoter LBD39/1-1991	GGGGACCACTTTGTACAAGAAAGCTGGGTATTCTTTTCCGAAATTTGA
attB1 SP/promoter LBD41/1-1988	GGGGACAAGTTTGTACAAAAAAGCAGGCTTAGCTTCCGTCTTTAGAGAT
attB2 ASP/promoter LBD41/1-1988	GGGGACCACTTTGTACAAGAAAGCTGGGTACTTTGGTTTCGATTATCT

Appendix 3: YFP pictures

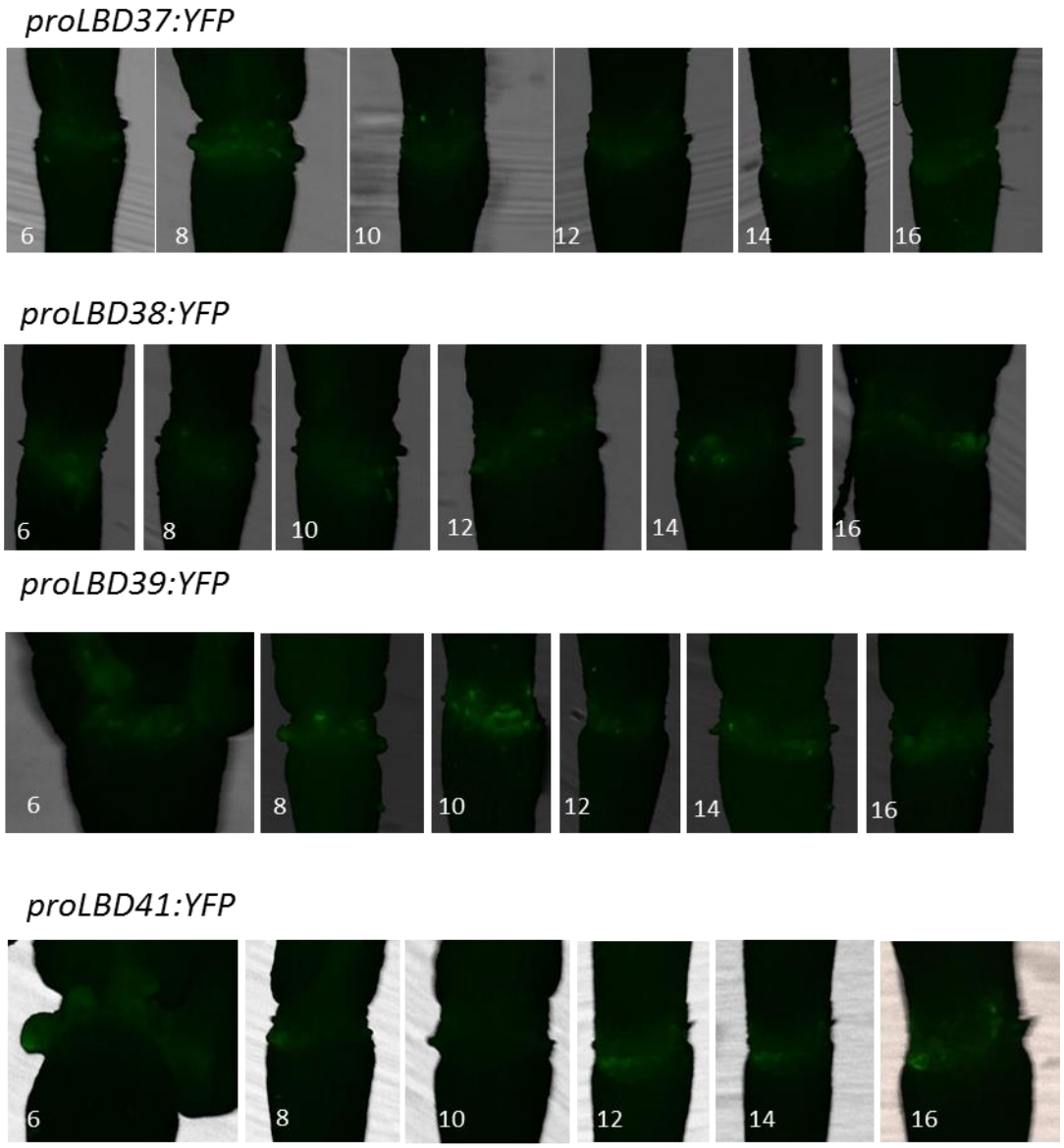

Supplemental figure 1: Pictures of YFP assessed LBD expression at the floral AZ, position 6-16.
The expression is quite weak, however all the YFP expression lines display YFP expression in the floral AZ the of all floral positions from 6-16 as seen in the *promoter:YFP* lines. (Position 2and 4 did not display a strong enough YFP expression for it to be captured by the camera.) *proLBD39:YFP* displays the strongest expression, especially at position 10. The expression seems to be located at the AZs of at the junction between the sepals, petals, filaments and the floral receptacle.

Appendix 4: SALK_lines

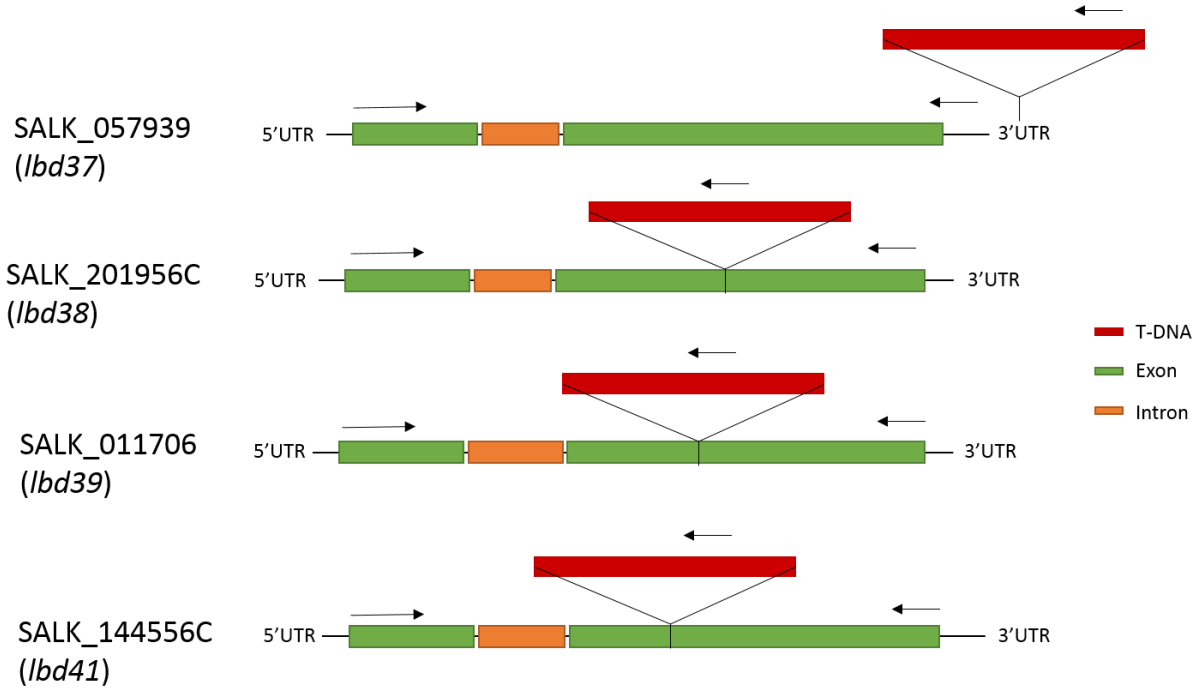

Supplemental figure 2: Demonstration of the T-DNA insertion in *LBD38*, *LBD39* and *LBD41* and the likely placement of the T-DNA in *LBD37*.

Appendix 5: GUS expression in seedlings

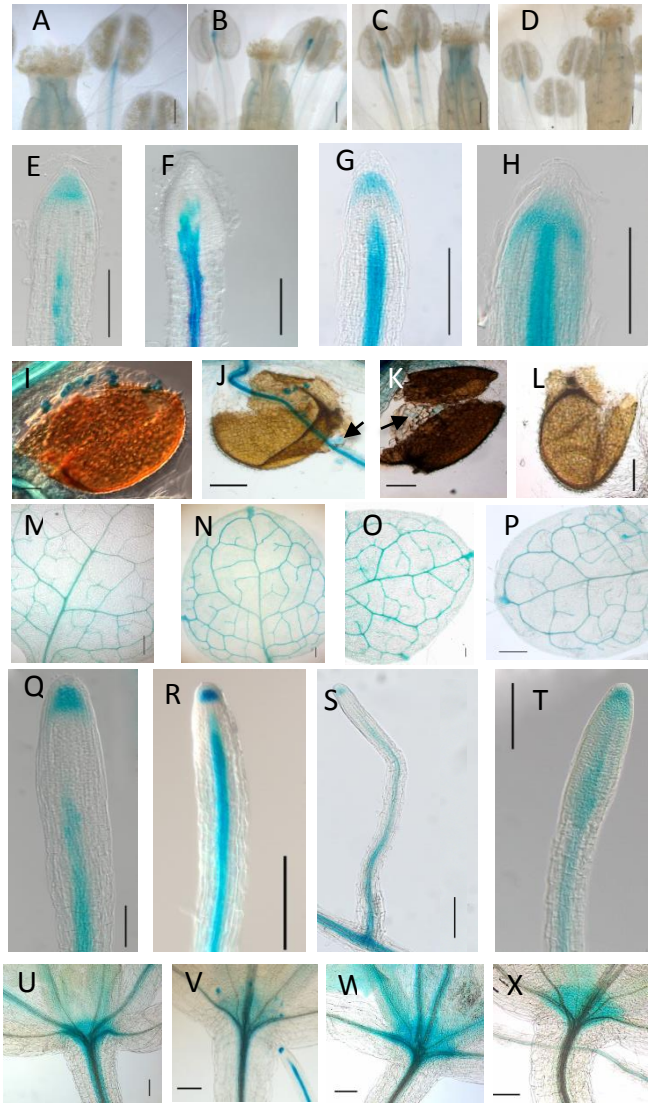

Supplemental figure 3: *proLBD37:GUS*, *proLBD38:GUS*, *proLBD39:GUS* and *proLBD41:GUS* expression in 12-day-old seedlings and full grown plant. A, E, I, M, Q, U shows *proLBD37:GUS* expression. B, F, J, N, R, V shows *proLBD38:GUS* expression. C, G, K, O, S, W shows *proLBD39:GUS* expression. D, H, L, P, T, X shows *proLBD41:GUS* expression.

(A) to **(D)** GUS expression in stamen and style
(E) to **(H)** GUS expression in the meristematic zone of the main root and in the main root tip
(I) to **(L)** GUS expression in the endosperm layer of the mature, germinated seed, except in the endosperm layer of the germinated *proLBD41:GUS* seed (L).
(M) to **(P)** GUS expression in the veins of young rosette leaves and in the hydratodes of the rosette leaves from *proLBD38:GUS, proLBD39:GUS* and *proLBD41:GUS* seedlings.
(Q) to **(T)** GUS expression in the meristematic zone of lateral roots and lateral root tip.
(U) to **(X)** GUS expression in the SAM.

Appendix 6: pBS of two *hae hsl2 lbd38 lbd39* mutants

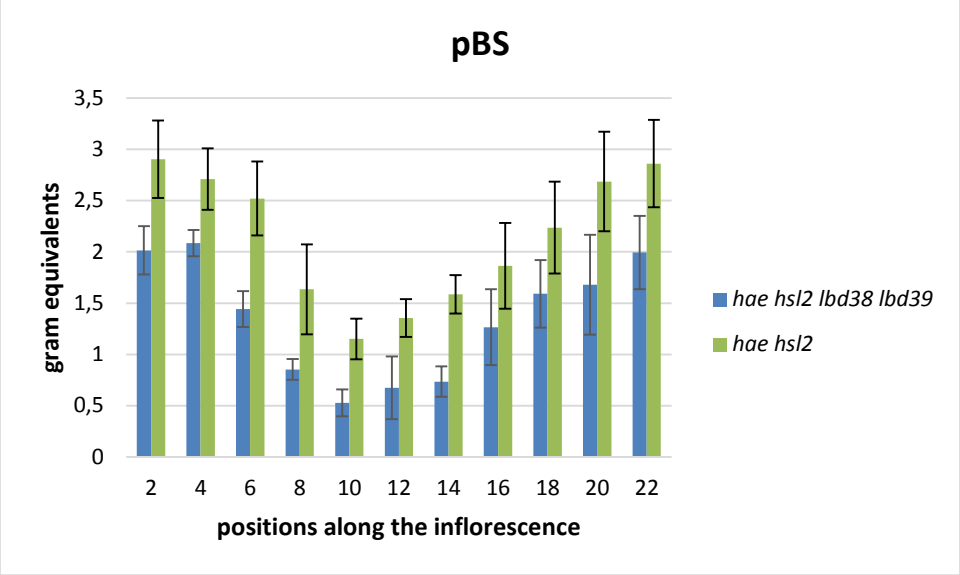

Supplemental figure 4: pBS of *hae hsl2 lbd38 lbd39.* This figure gives an indication of how the additional loss *of LBD38 LBD39* effect *hae hsl2*. From the pBS measurements of the two *hae hsl2 lbd38 lbd39* mutants it may seem as if there is a partial rescue of *hae hsl2* by *lbd38 lbd39*. There is a significant reduction from position 2 to position 10. The highest significant differences between *hae hsl2* and *hae hsl2* by *lbd38 lbd39* were at position 6 and 8 correlating with the timing of abscission (For T-test se below.)

T-test	
positions	P-value
2	0,00186096
4	0,00011191
6	2,4793E-05
8	1,0682E-05
10	0,0005007
12	0,03347604
14	0,00033323
16	0,05427936
18	0,03408849
20	0,01035993
22	0,01387807

Supplemental table 2: T-test. The P values from the T-test when comparing the pBS values of *hae hsl2* to *hae hsl2 lbd38 lbd39* in order to investigate any significant differences between the two mutant lines.